

## Supporting information:

# Peripherally Diketopyrrolopyrrole-Functionalized Dendritic Oligothiophenes – Synthesis, Molecular Structure, Properties and Applications

Wei Gao,<sup>a,e</sup> Qun Luo,<sup>a</sup> Junkai Wang,<sup>b</sup> Yi Lin,<sup>c</sup> Changquan Tang,<sup>d</sup> Junyan Dou,<sup>a</sup> Hongwei

Tan,<sup>b</sup> Qingdong Zheng,<sup>d</sup> Chang-Qi Ma,\*<sup>a</sup> Zheng Cui<sup>a</sup>

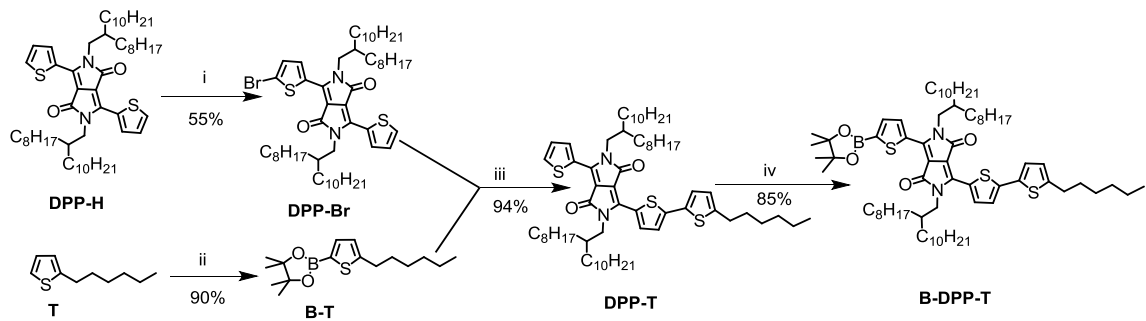
*a Printable Electronics Research Center; Suzhou Institute of Nano-Tech and  
Nano-Bionics, Collaborative Innovation Center of Suzhou Nano Science and  
Technology, Chinese Academy of Sciences, 398 Ruoshui Road, SEID SIP, Suzhou,  
Jiangsu 215123, PR China.*

*b College of Chemistry, Beijing Normal University, No. 19, XinJieKouWai St.,  
HaiDian District, Beijing, 100875, PR China*

*c Department of Chemistry, Xi'an Jiaotong Liverpool University, 111 Ren Ai Road,  
SEID SIP, Suzhou, 215123, P. R. China*

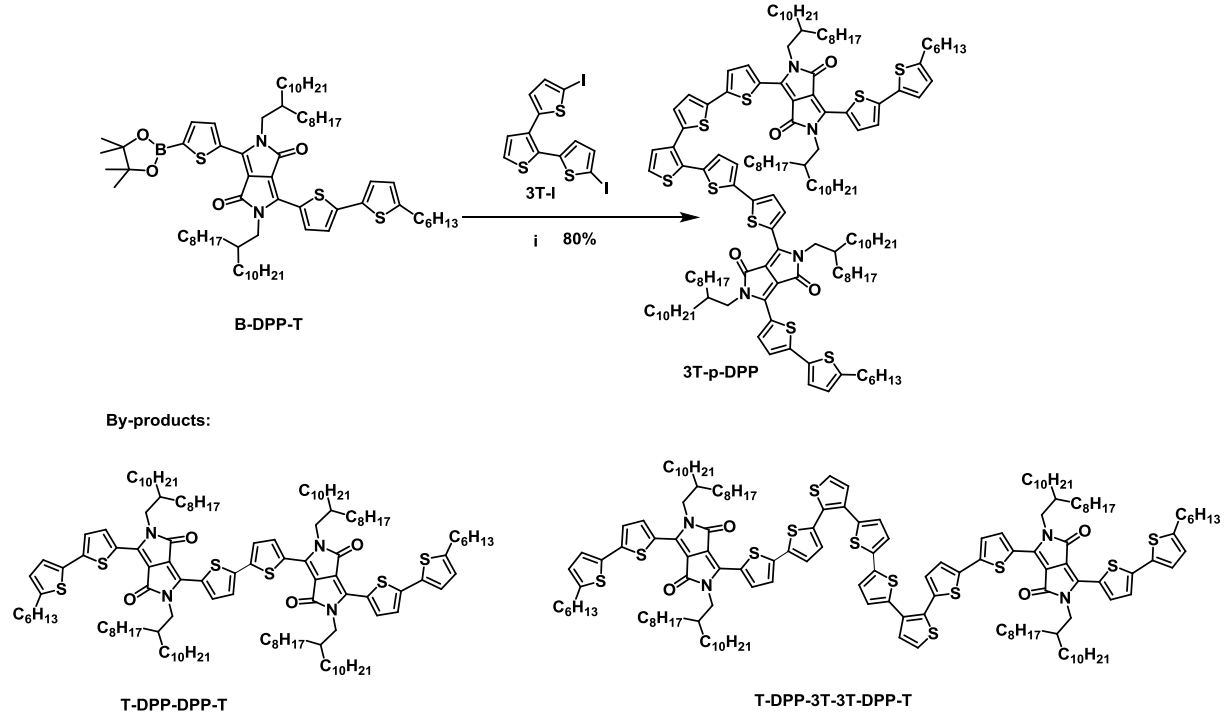
*d State Key Laboratory of Structure Chemistry, Fujian Institute of Research on the  
Structure of Matter, Chinese Academy of Sciences, 155 Yangqiao West Road, Fuzhou,  
Fujian 350002, P. R. China*

*e University of Chinese Academy of Sciences, Beijing, 100049, P. R. China*



**Scheme S1.** Synthetic route to the key precursor **B-DPP-T**.

Reagents and conditions: i) NBS (1.1 eq), CHCl<sub>3</sub>; ii) 1. *n*-BuLi/THF, 2. 2-isopropoxy-4,4,5,5-tetramethyl-1,3,2-dioxaborolane; iii) [Pd<sub>2</sub>(dba)<sub>3</sub>] CHCl<sub>3</sub>, HP(*t*Bu)<sub>3</sub>BF<sub>4</sub>, K<sub>2</sub>CO<sub>3</sub>, THF; iv) [Ir(OMe)(COD)]<sub>2</sub>, dtbpy, HBpin, THF. (dba=dibenzylideneacetone; COD = 1,5-cyclooctadiene; dtbpy = 4,4'-di-*tert*-butyl-2,2'-bipyridine).



**Scheme S2.** Synthesis of first-generation dendrons **3T-p-DPP**.

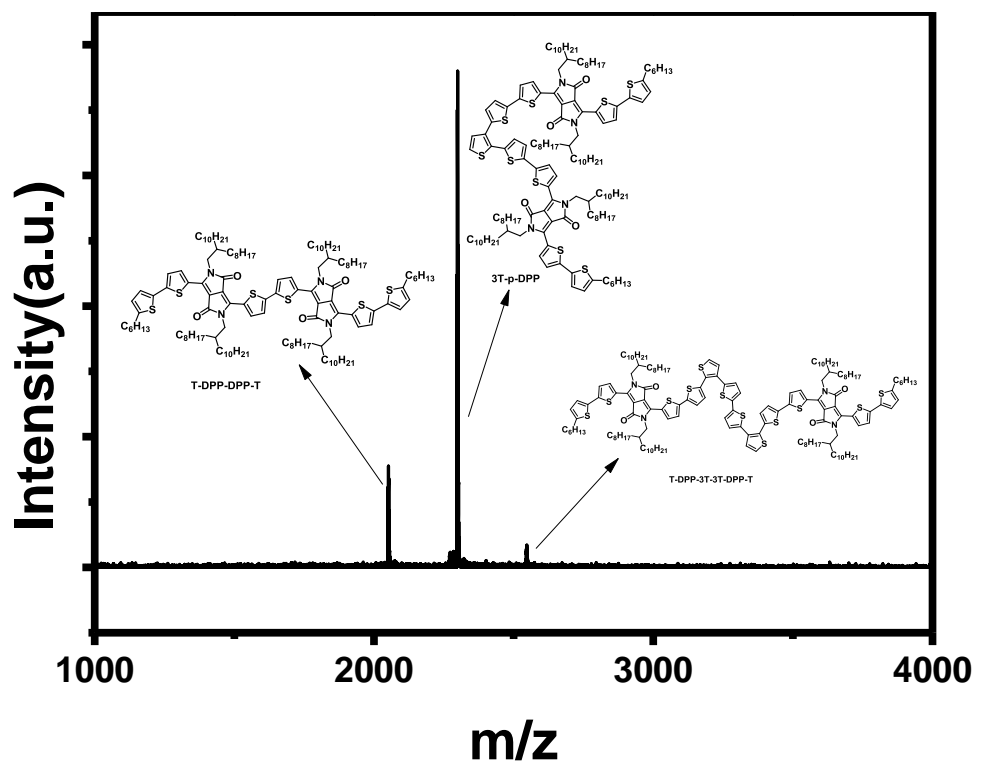
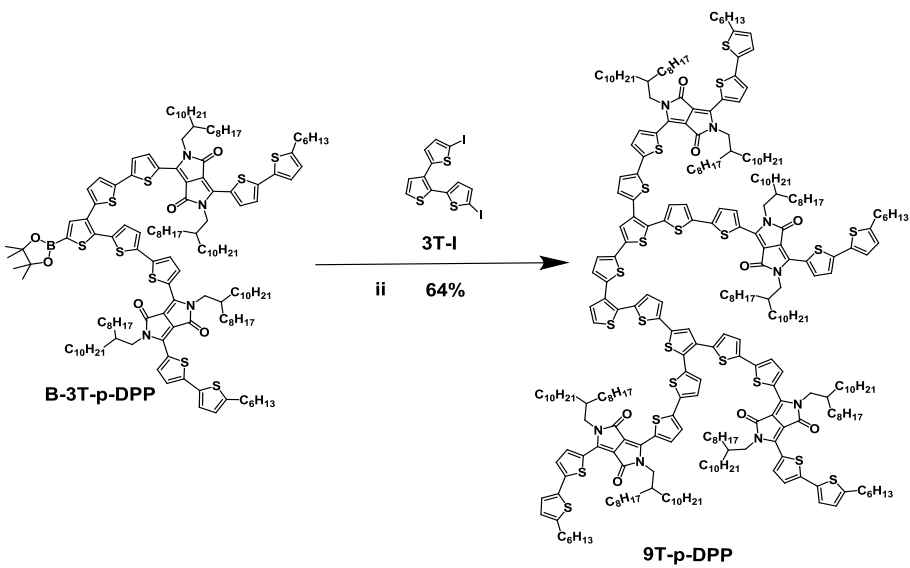
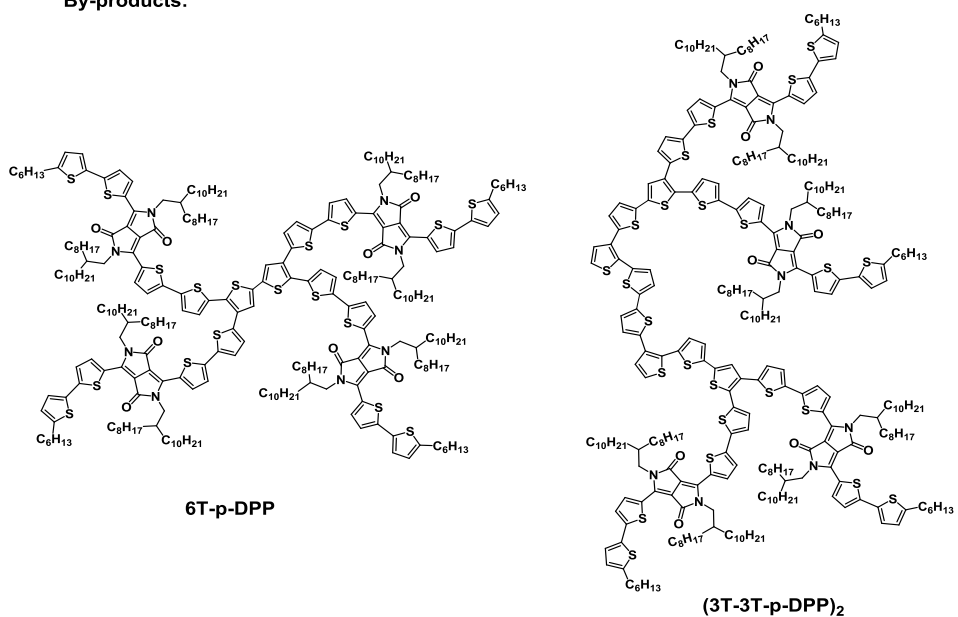


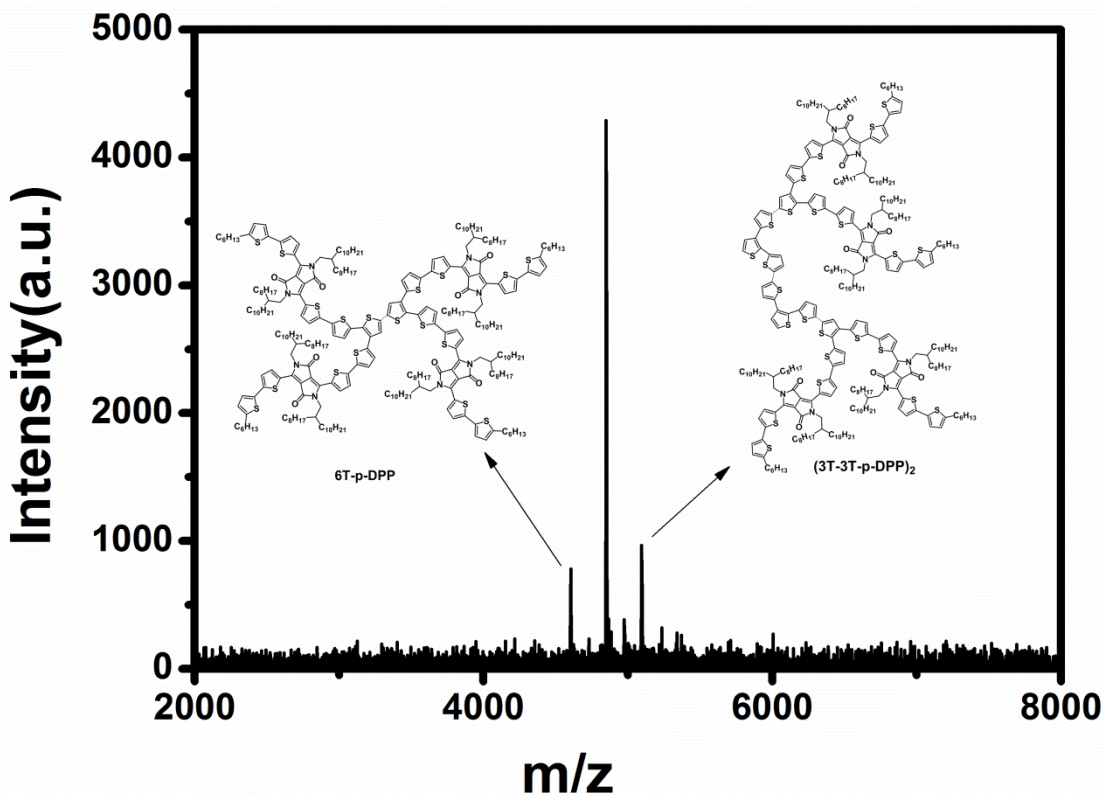
**Figure S1.** MALDI-TOF Mass-spectrometric characterization of **3T-p-DPP** and corresponding by-products (T-DPP-DPP-T and T-DPP-3T-3T-DPP-T).



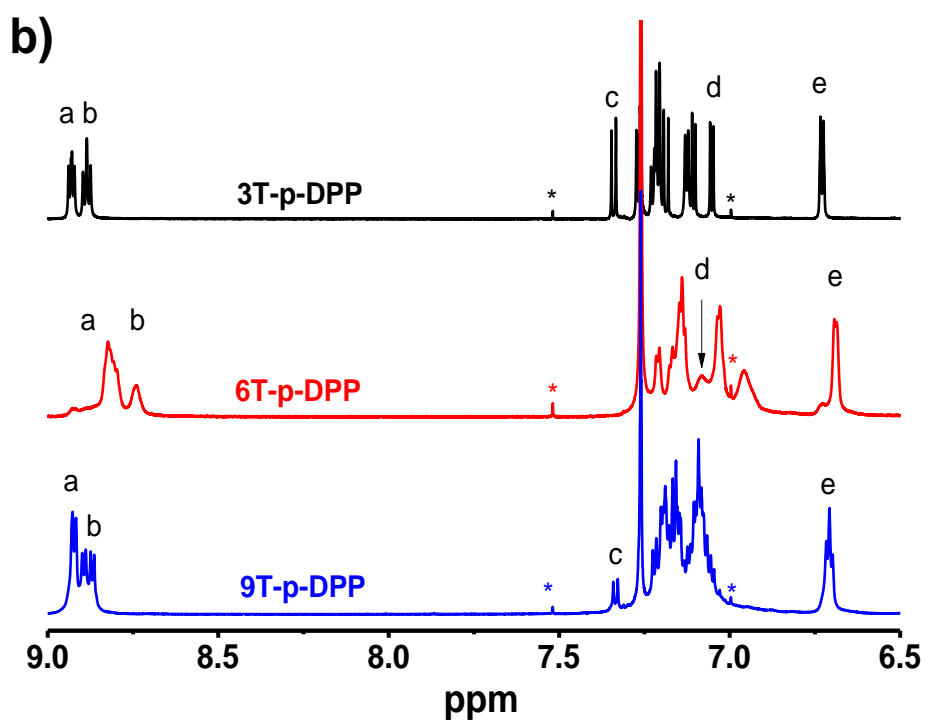
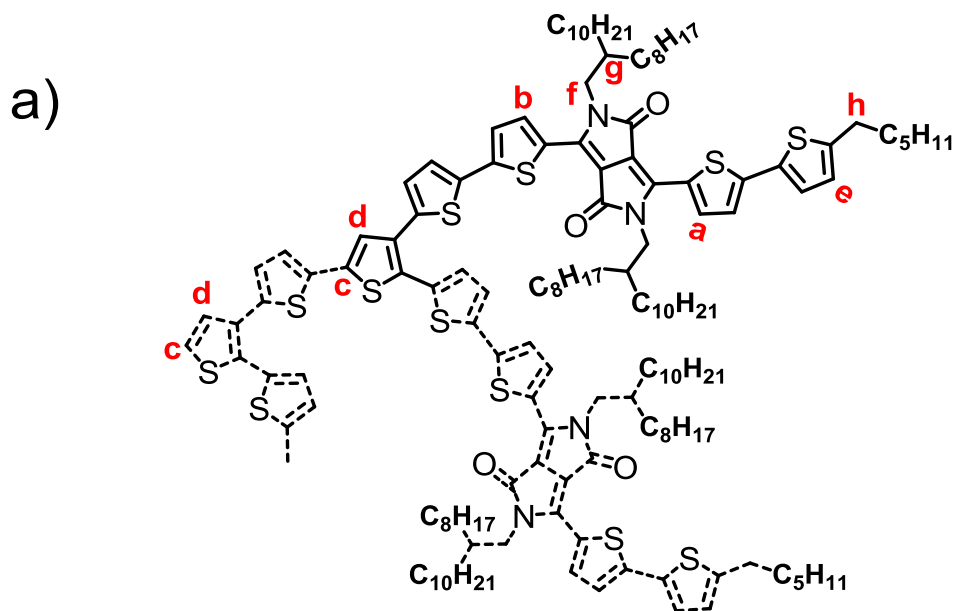
**By-products:**



**Scheme S3.** Synthesis of second-generation dendrons **9T-p-DPP** by using **B-3T-p-DPP** and **3T-I**.



**Figure S2.** MALDI-TOF Mass-spectrometric characterization of **9T-p-DPP** and corresponding by-products (**6T-p-DPP** and  $(3T\text{-}3T\text{-}p\text{-DPP})_2$ ).



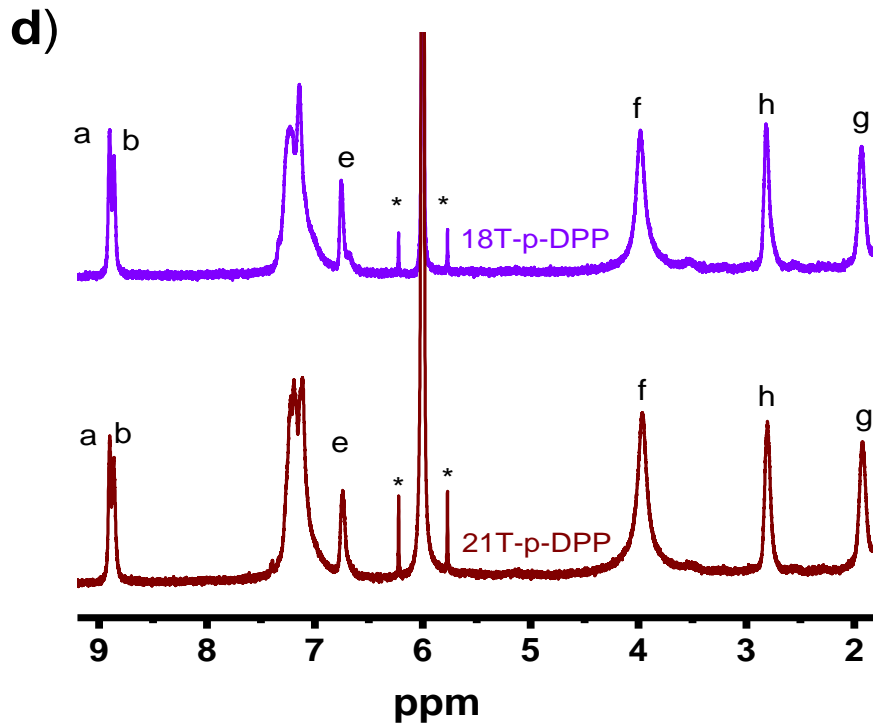
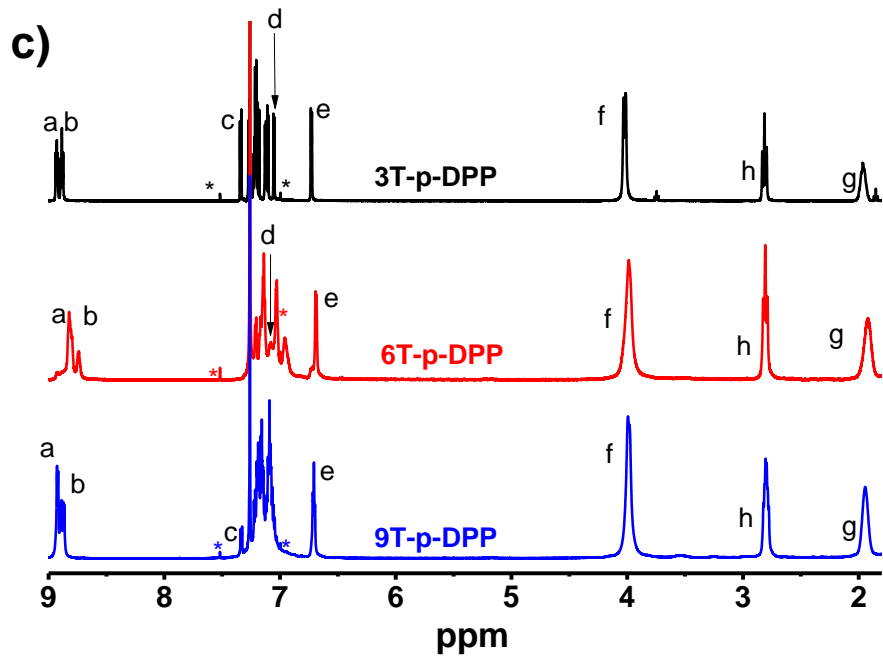
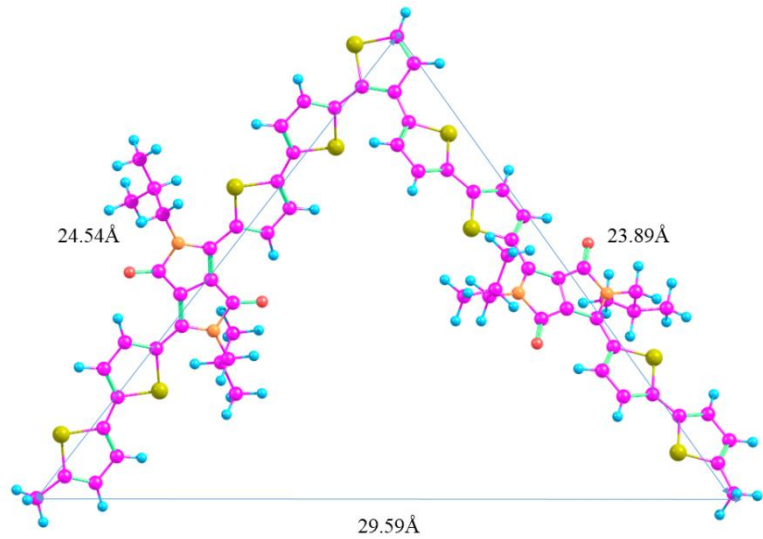
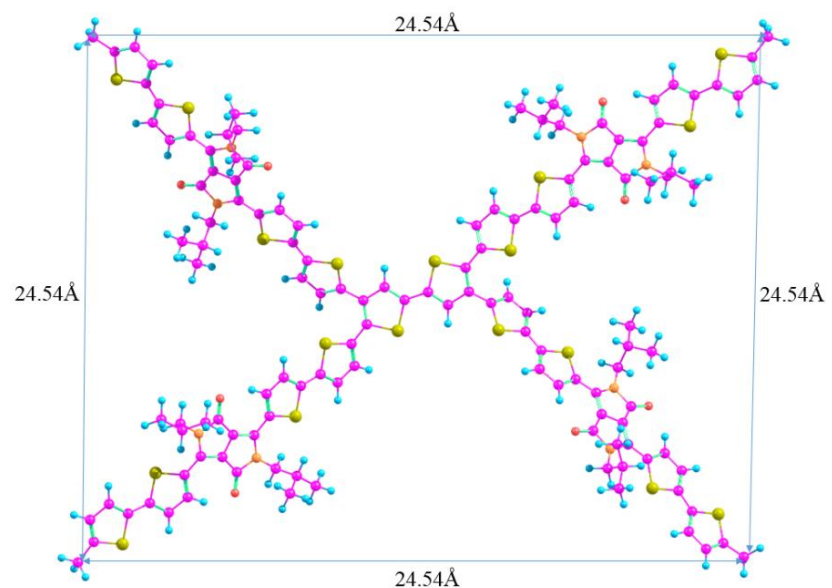


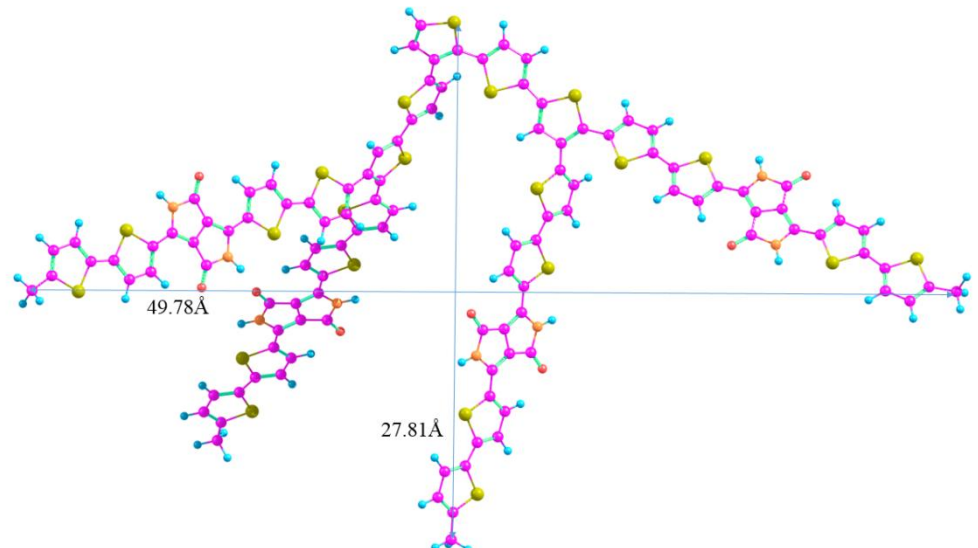
**Figure S3.** a) Chemical structure representation of DOT-p-DPPs; b)  $^1\text{H}$  NMR spectra of **3T-p-DPP**, **6T-p-DPP**, **9T-p-DPP** in the aromatic range; c)  $^1\text{H}$  NMR spectra of **3T-p-DPP**, **6T-p-DPP** and **9T-p-DPP** in  $\text{CDCl}_3$ ; c)  $^1\text{H}$  NMR spectra of **18T-p-DPP** and **21T-p-DPP** in  $\text{C}_2\text{D}_2\text{Cl}_4$  (two single peaks marked with \* are the C-H coupling peak of the  $\text{CDCl}_3$  or  $\text{C}_2\text{D}_2\text{Cl}_4$ ).



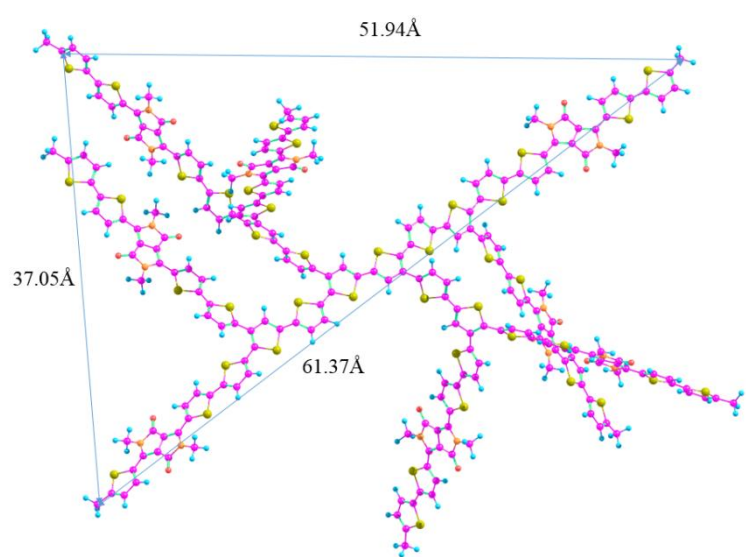
3T-p-DPP



6T-p-DPP



9T-p-DPP



18T-p-DPP

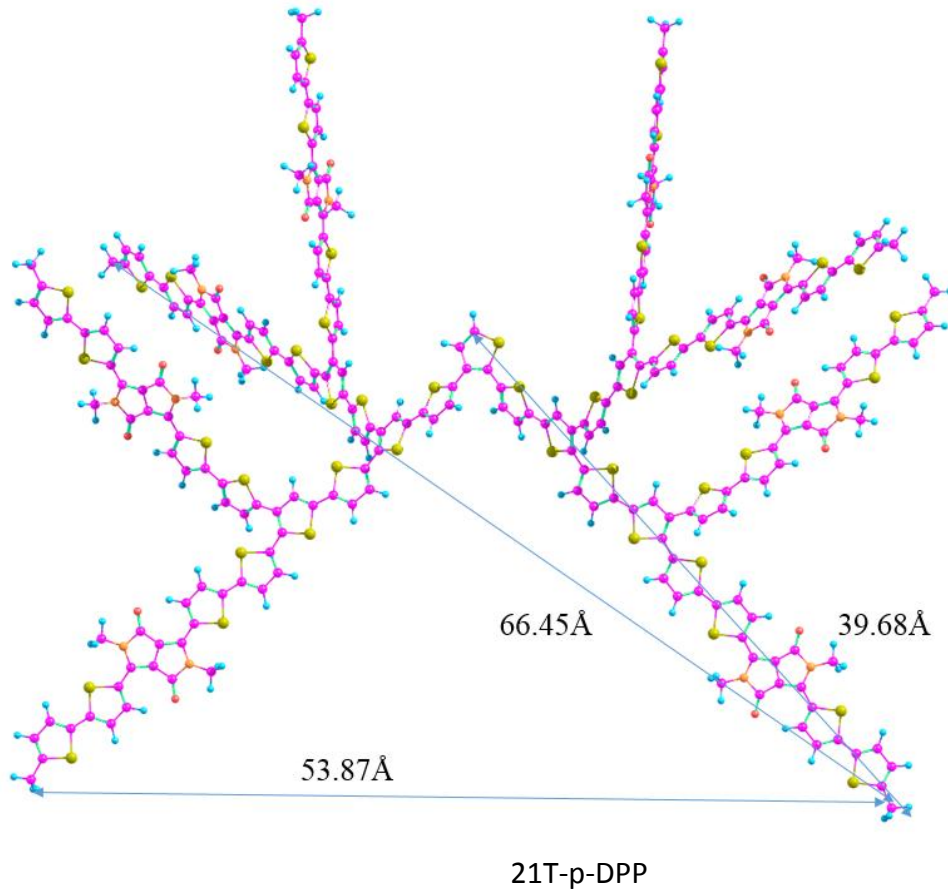


**Figure S4.** Molecular size of DOT-p-DPPs by molecular simulation.

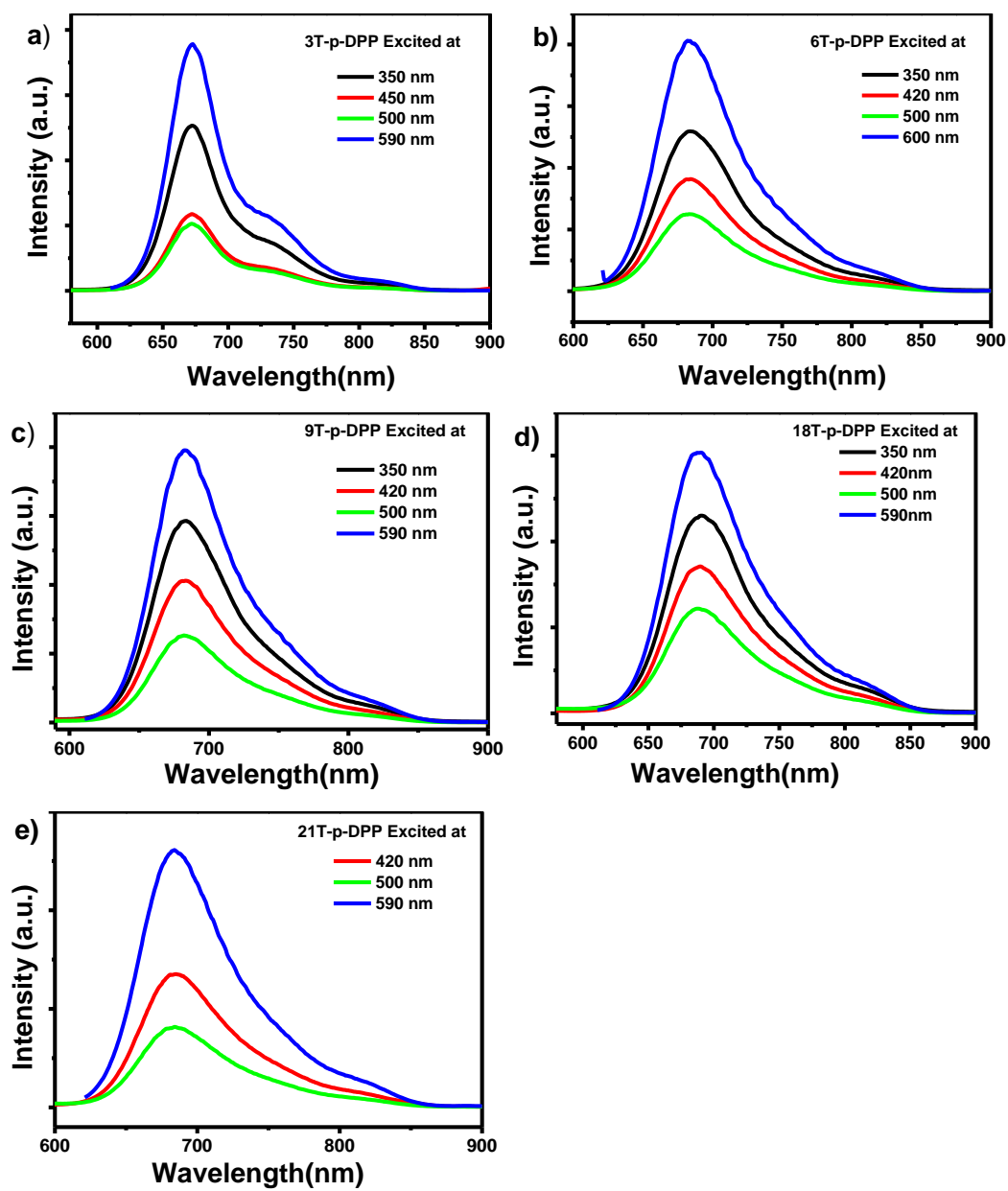


**Figure S5.** Emission spectra of DOT-p-DPPs measured at different excitation wavelengths.

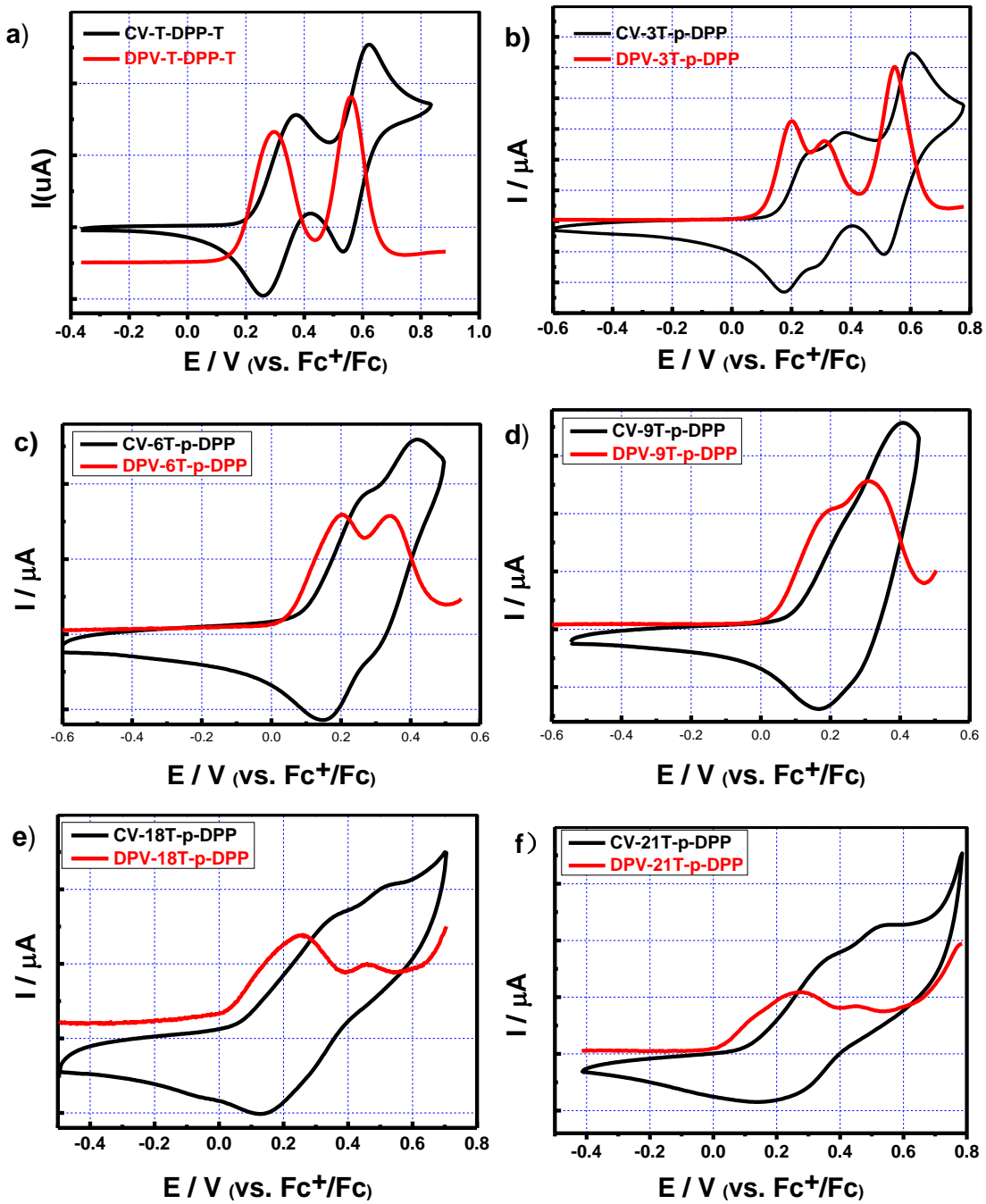


**Figure S6.** a, b, c, d) CV and DPV of T-DPP-T, 3T-p-DPP, 6T-p-DPP, 9T-p-DPP at  $1 \times 10^{-3} \text{ mol} \cdot \text{L}^{-1}$  in  $\text{CH}_2\text{Cl}_2$  TBAPF<sub>6</sub>(0.1 M), room temperature,  $V = 100 \text{ mV s}^{-1}$ ; e) 18T-p-DPP at  $5 \times 10^{-4} \text{ mol} \cdot \text{L}^{-1}$  in  $\text{CH}_2\text{Cl}_2$ , room temperature, TBAPF<sub>6</sub>(0.1 M),  $V = 100 \text{ mV s}^{-1}$ ; f) 21T-p-DPP at  $2.5 \times 10^{-4} \text{ mol} \cdot \text{L}^{-1}$  in  $\text{CH}_2\text{Cl}_2$ , room temperature, TBAPF<sub>6</sub>(0.1 M),  $V = 100 \text{ mV s}^{-1}$

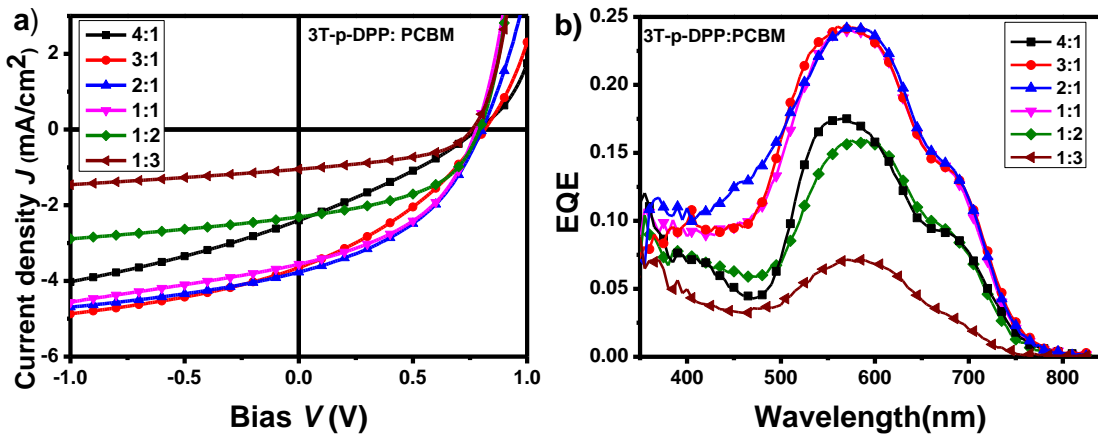


Figure S7. a) J–V curves for BHJ solar cells with varying ratios of 3T-p-DPP and PC<sub>61</sub>BM under illumination (nominal AM1.5G, 100 mW cm<sup>-2</sup>) and b) EQE spectra of the corresponding devices.

Table S1. Summary of device performance for BHJ solar cells with varying ratios of 3T-p-DPP and PC<sub>61</sub>BM

D:A (solvent)	Thickness (nm)	$J_{SC}$ [mA cm <sup>-2</sup> ]	$V_{OC}$ [V]	FF	Mpp
4:1	180	2.40	0.78	0.30	0.56
3:1	142	3.65	0.81	0.34	1.01
2:1	106	3.77	0.80	0.41	1.24
1:1	110	3.56	0.78	0.44	1.22
1:2	103	2.31	0.79	0.48	0.88
1:3	230	1.05	0.76	0.47	0.38

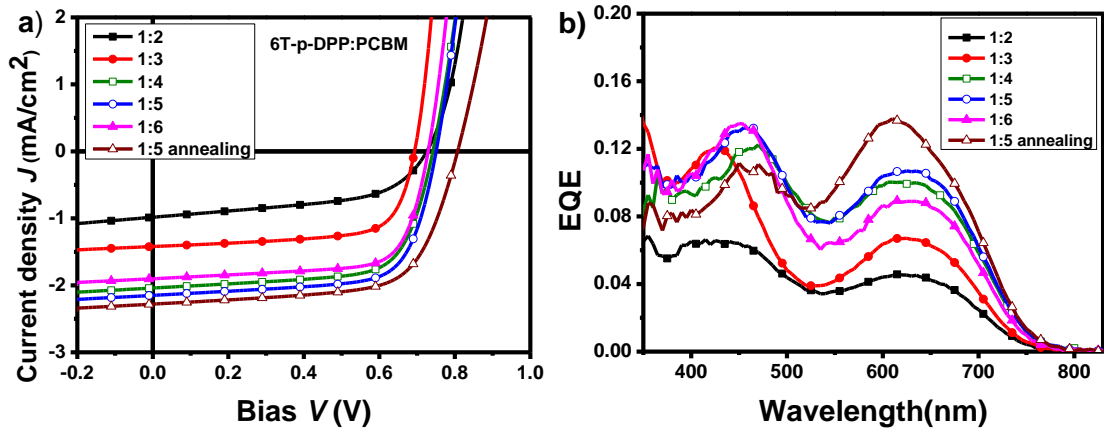


Figure S8. a) J–V curves for BHJ solar cells with varying ratios of 6T-p-DPP and  $\text{PC}_{61}\text{BM}$  under illumination (nominal AM1.5G,  $100 \text{ mW cm}^{-2}$ ) and b) EQE spectra of the corresponding devices.

Table S2. Summary of device performance for BHJ solar cells with varying ratios of 6T-p-DPP and  $\text{PC}_{61}\text{BM}$

D:A (solvent)	Thickness (nm)	$J_{SC}$ [mA cm $^{-2}$ ]	$V_{OC}$ [V]	FF	Mpp
1:2	80	0.98	0.73	0.53	0.38
1:3	94	1.42	0.69	0.69	0.68
1:4	84	2.04	0.74	0.69	1.04
1:5	90	2.15	0.75	0.70	1.13
1:6	83	1.9	0.73	0.71	0.98
1:5(annealing)	90	2.28	0.81	0.67	1.24

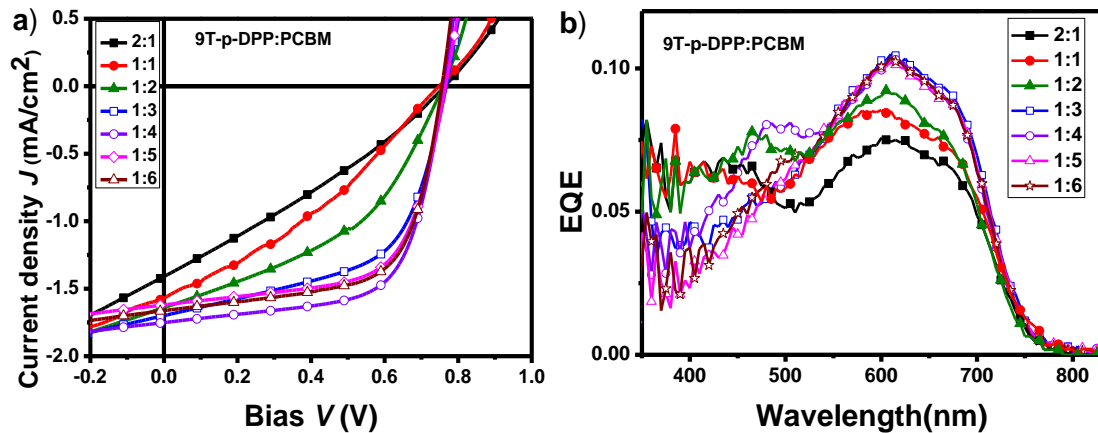


Figure S9. a) J–V curves for BHJ solar cells with varying ratios of 9T-p-DPP and PC<sub>61</sub>BM under illumination (nominal AM1.5G, 100 mW cm $^{-2}$ ) and b) EQE spectra of the corresponding devices.

Table S3. Summary of device performance for BHJ solar cells with varying ratios of 9T-p-DPP and PC<sub>61</sub>BM

D:A (solvent)	Thickness (nm)	$J_{SC}$ [mA cm $^{-2}$ ]	$V_{OC}$ [V]	FF	Mpp
2:1	129	1.41	0.77	0.31	0.34
1:1	153	1.57	0.75	0.33	0.39
1:2	80	1.64	0.76	0.43	0.54
1:3	94	1.7	0.77	0.56	0.73
1:4	84	1.75	0.76	0.65	0.86
1:5	90	1.62	0.77	0.64	0.80
1:6	83	1.66	0.76	0.65	0.82

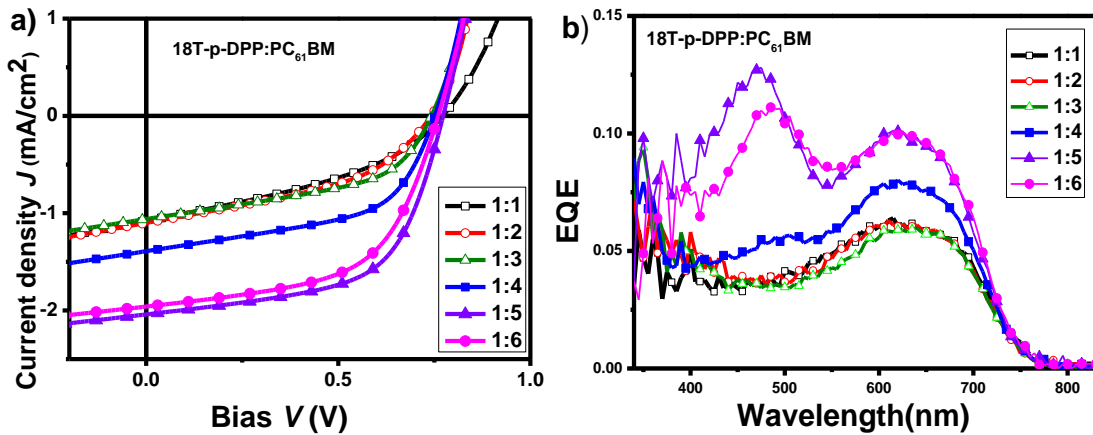


Figure S10. a) J–V curves for BHJ solar cells with varying ratios of 18T-p-DPP and PC<sub>61</sub>BM under illumination (nominal AM1.5G, 100 mW cm $^{-2}$ ) and b) EQE spectra of the corresponding devices.

Table S4. Summary of device performance for BHJ solar cells with varying ratios of 18T-p-DPP and PC<sub>61</sub>BM

D:A (solvent)	Thickness (nm)	$J_{SC}$ [mA cm $^{-2}$ ]	$V_{OC}$ [V]	FF	Mpp
1:1	112	1.08	0.77	0.38	0.32
1:2	104	1.10	0.74	0.43	0.35
1:3	104	1.06	0.74	0.49	0.38
1:4	95	1.39	0.75	0.54	0.56
1:5	84	2.04	0.77	0.59	0.93
1:6	90	1.96	0.76	0.56	0.83

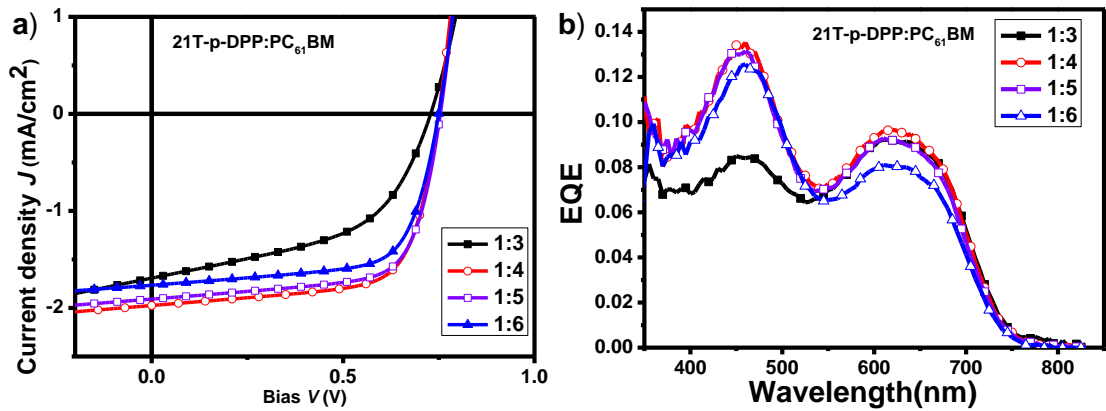


Figure S11. a) J–V curves for BHJ solar cells with varying ratios of 21T-p-DPP and PC $_{61}$ BM under illumination (nominal AM1.5G, 100 mW cm $^{-2}$ ) and b) EQE spectra of the corresponding devices.

Table S5. Summary of device performance for BHJ solar cells with varying ratios of 21T-p-DPP and PC $_{61}$ BM

D:A (solvent)	Thickness (nm)	$J_{SC}$ [mA cm $^{-2}$ ]	$V_{OC}$ [V]	FF	Mpp
1:3	86	1.69	0.73	0.51	0.63
1:4	81	1.97	0.75	0.69	1.02
1:5	74	1.91	0.75	0.69	0.99
1:6	79	1.76	0.74	0.70	0.91

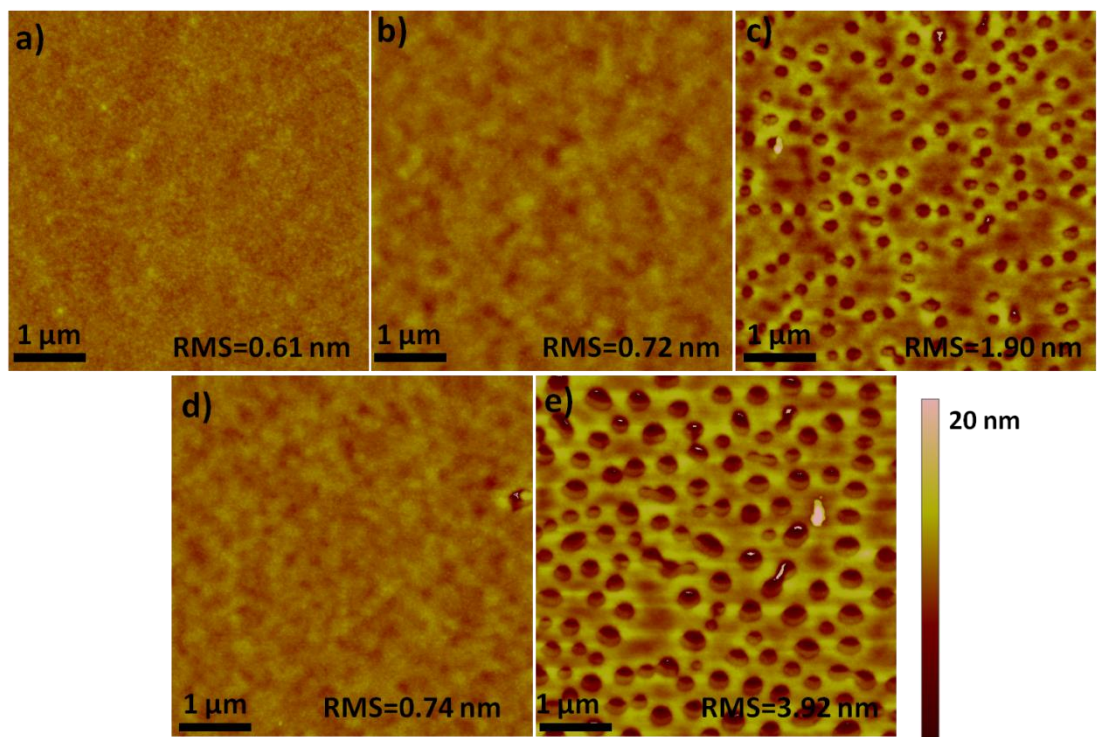


Figure S12. AFM height images of DOT-p-DPP:PC<sub>61</sub>BM blend film. a)3T-p-DPP; b) 6T-p-DPP; c) 9T-p-DPP; d) 18T-p-DPP; e) 21T-p-DPP. The scan area of all images was 5 × 5 μm.

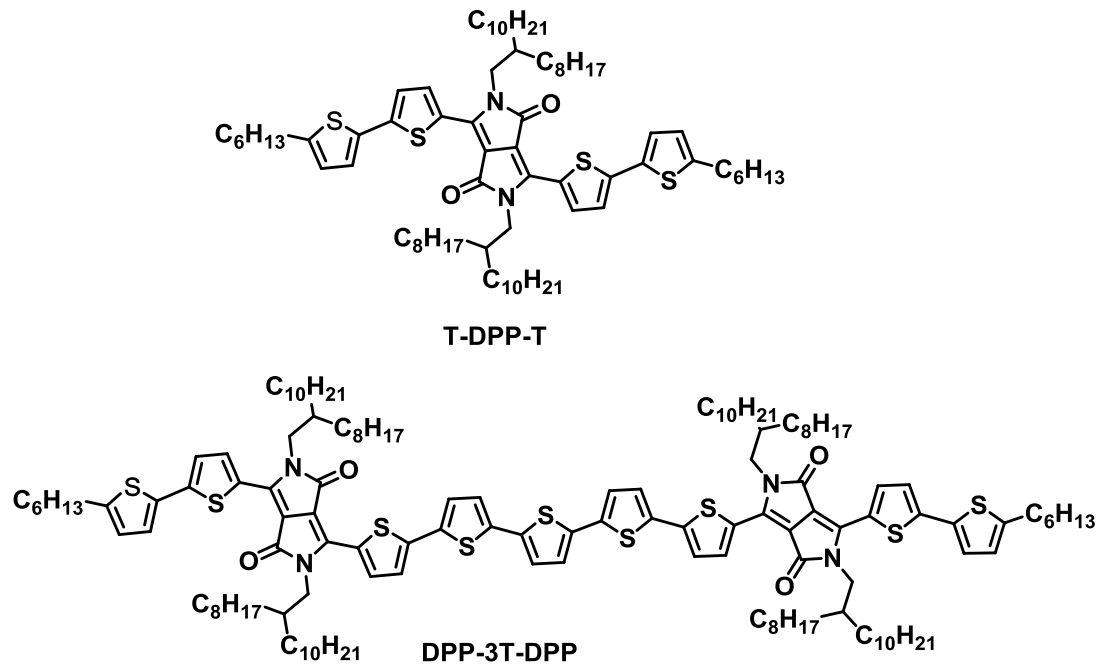
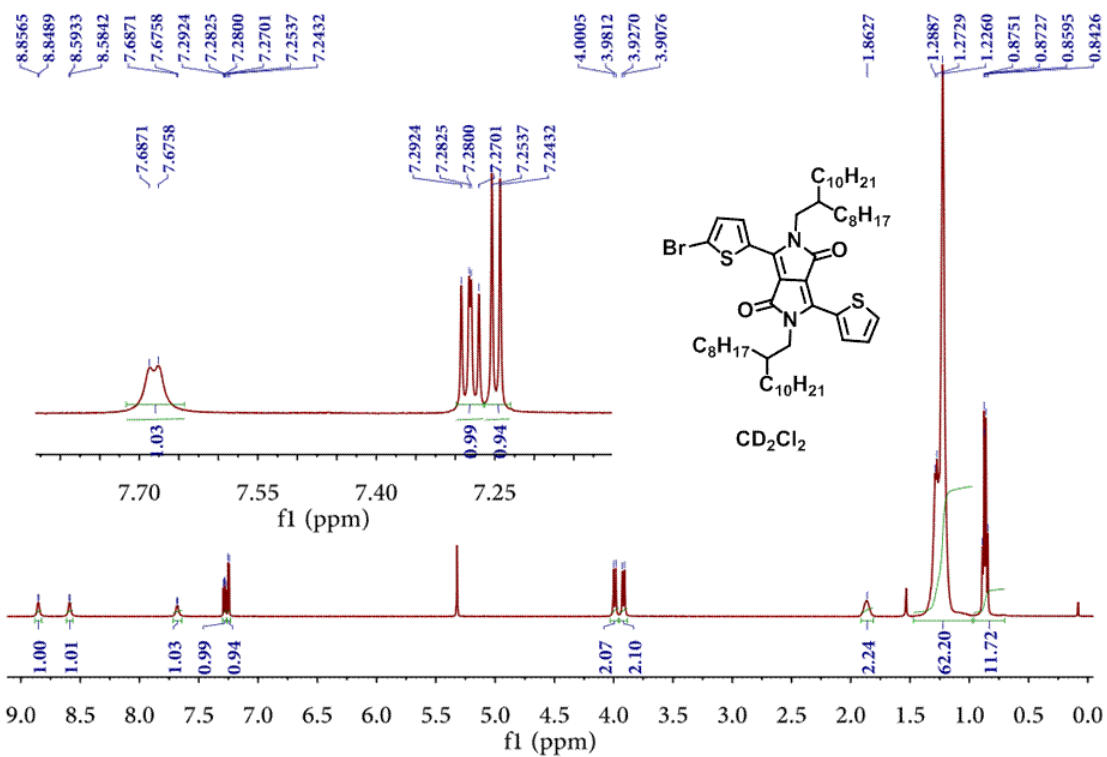
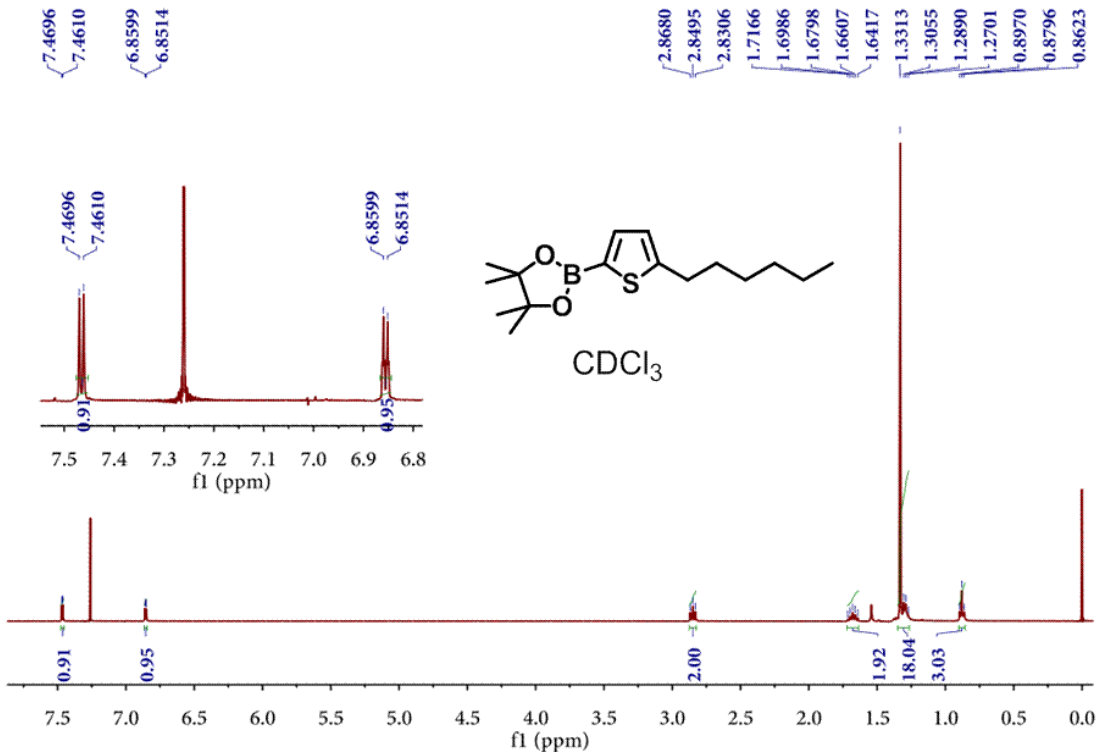


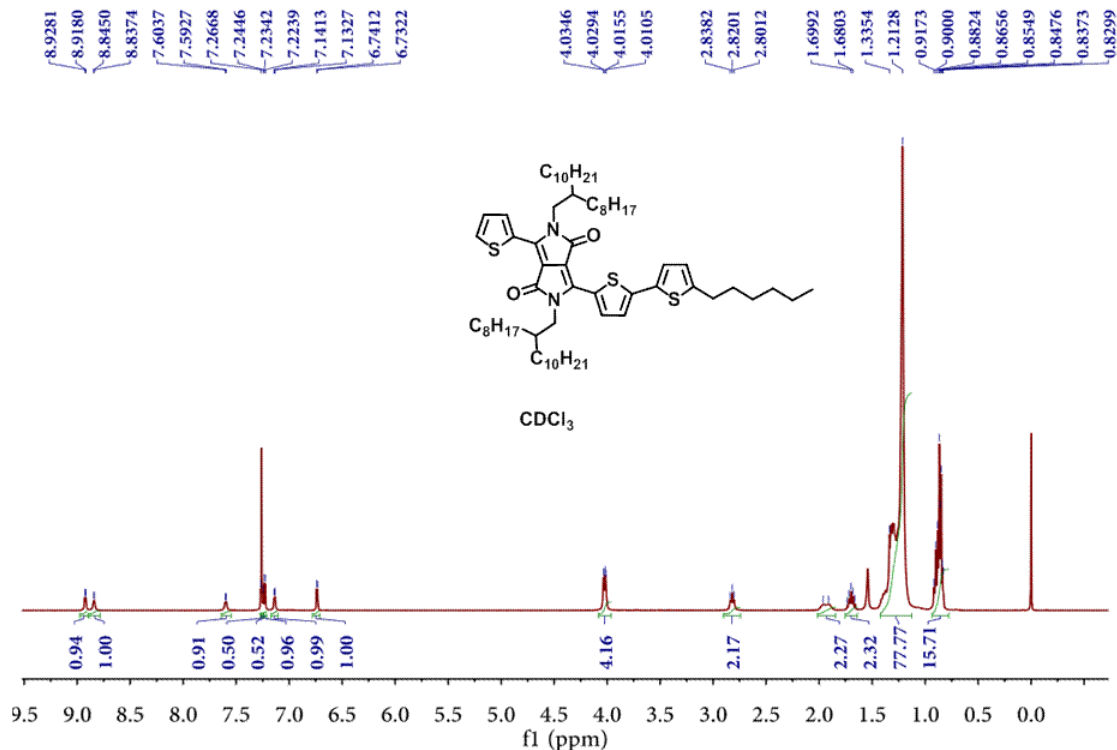
Figure S13. Chemical structure representation of T-DPP-T,DPP-3T-DPP.



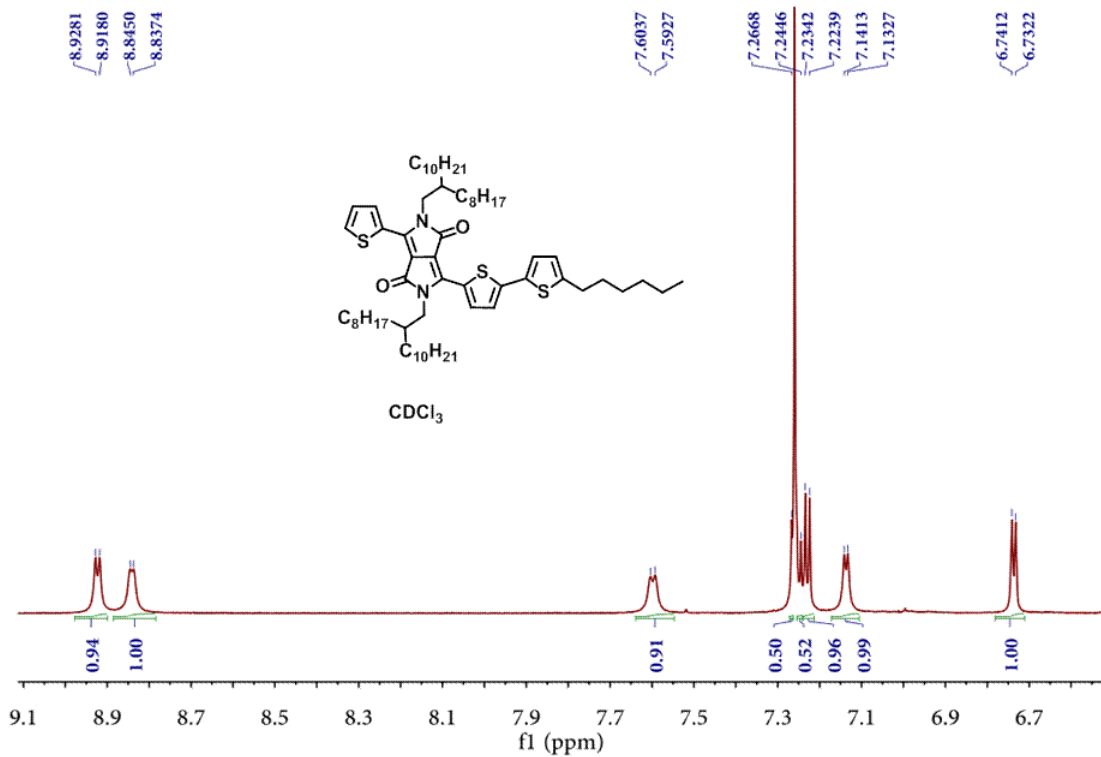
<sup>1</sup>H NMR of DPP-Br



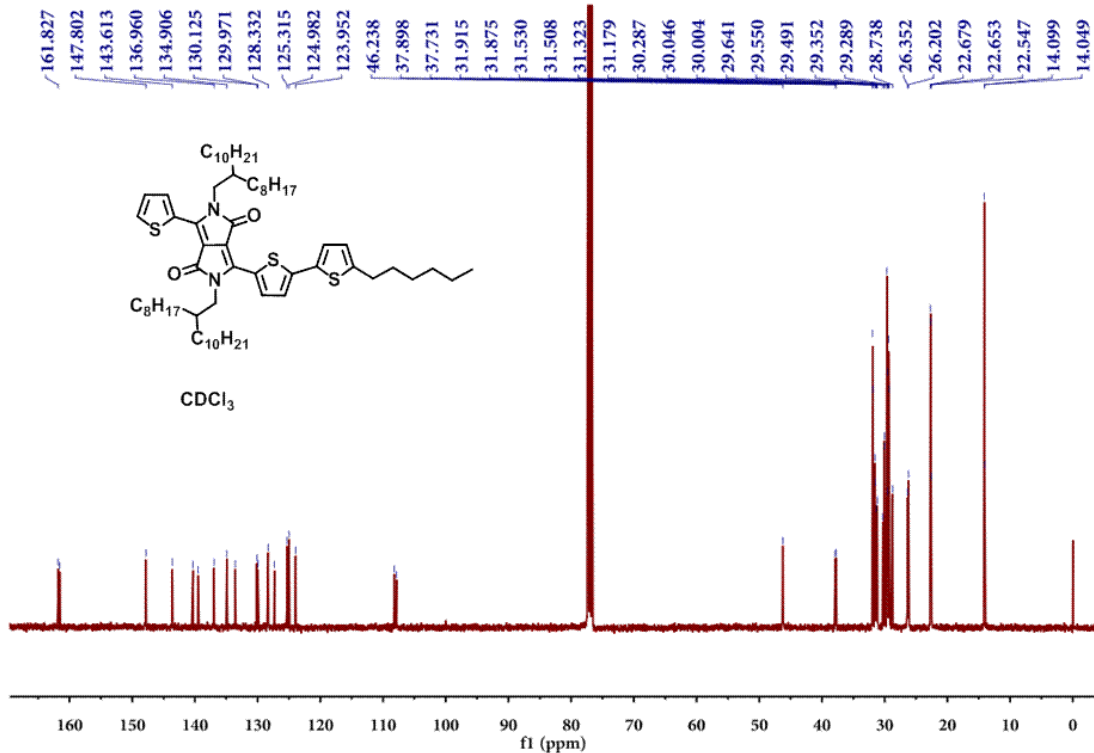
<sup>1</sup>H NMR of B-T



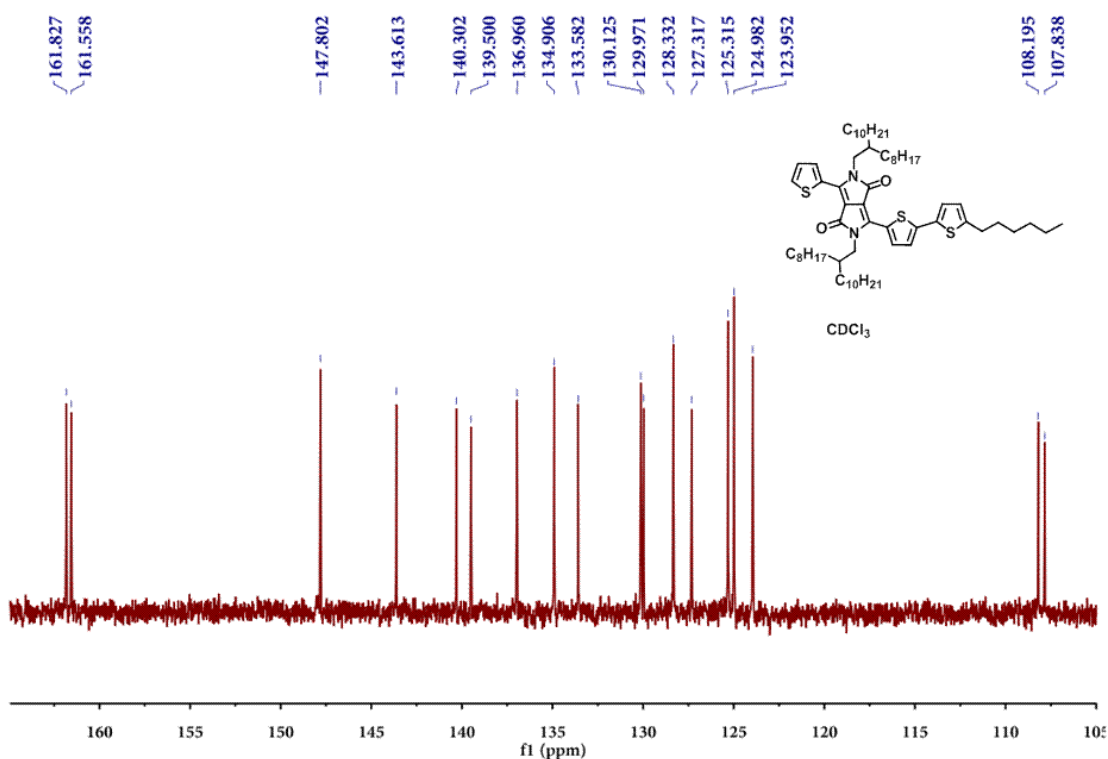
$^1\text{H}$  NMR of **DPP-T**



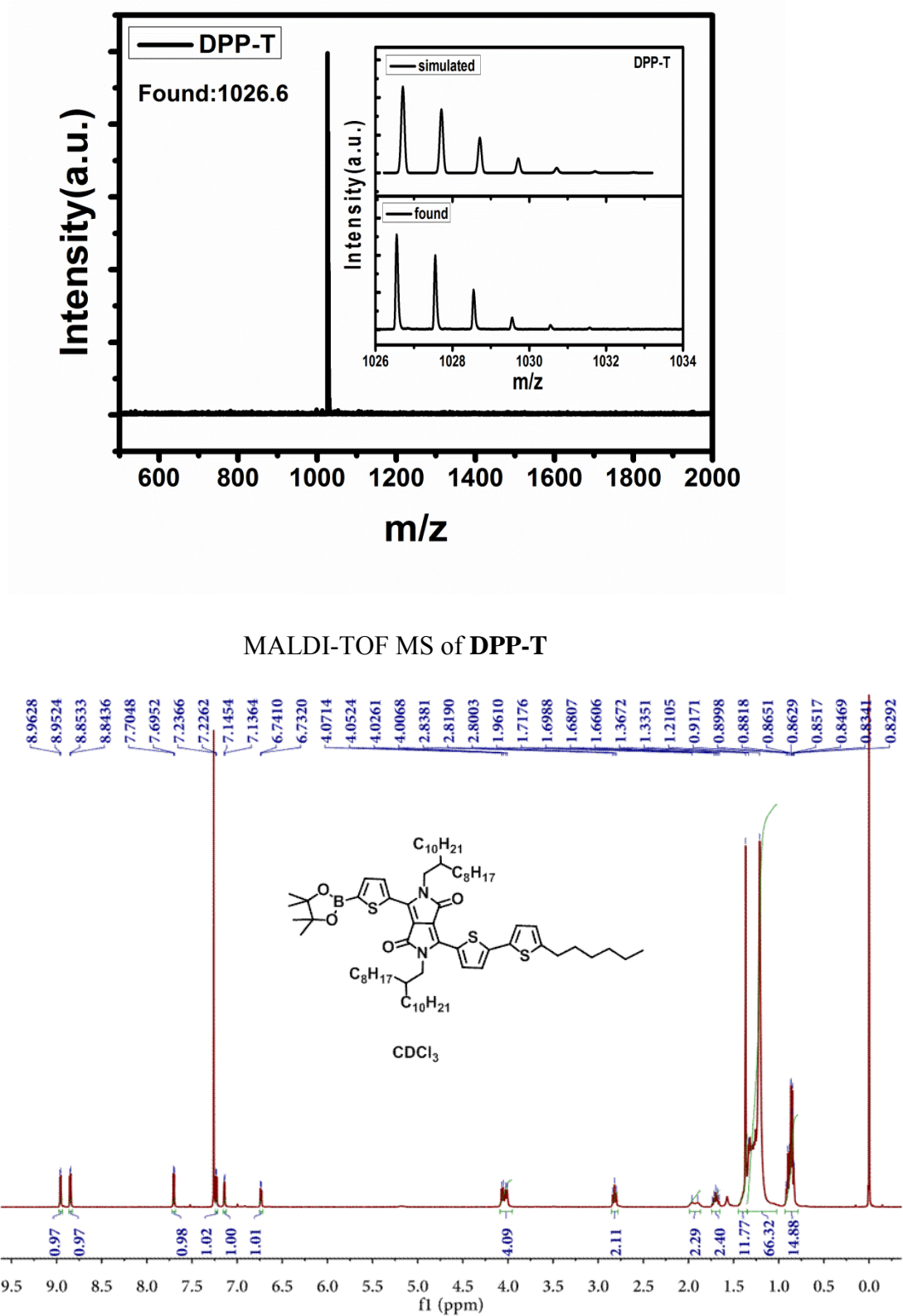
$^1\text{H}$  NMR of **DPP-T** (Zoom)



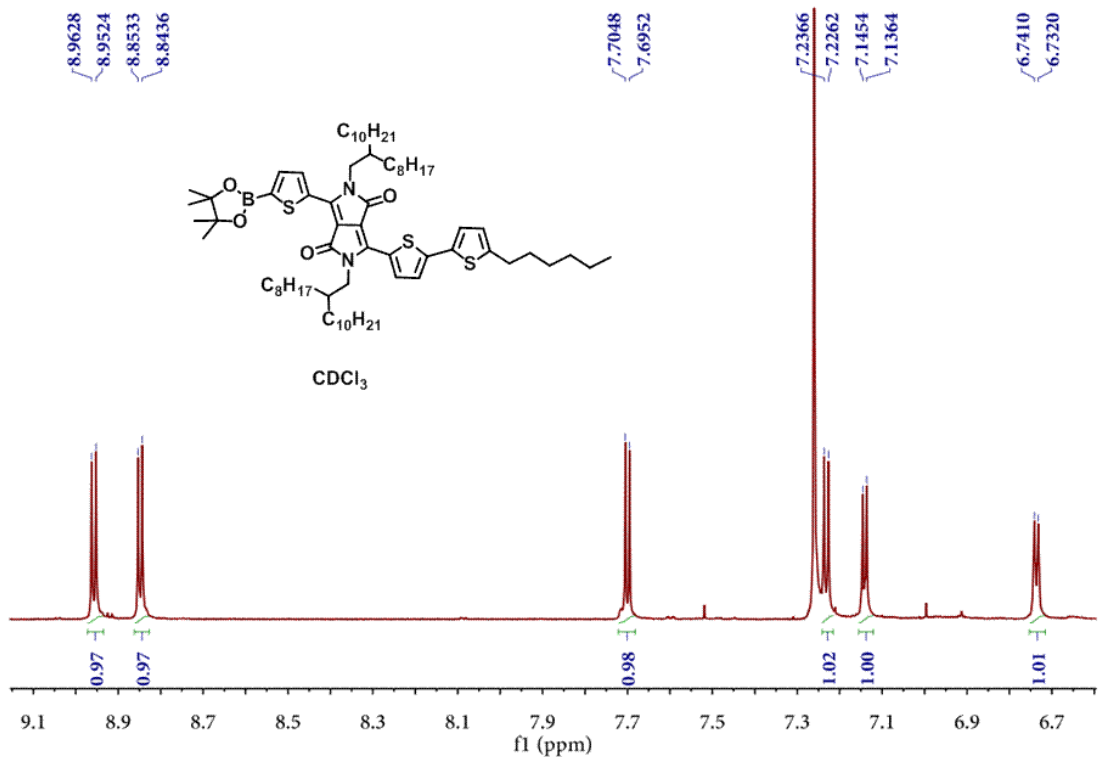
### <sup>13</sup>C NMR of DPP-T



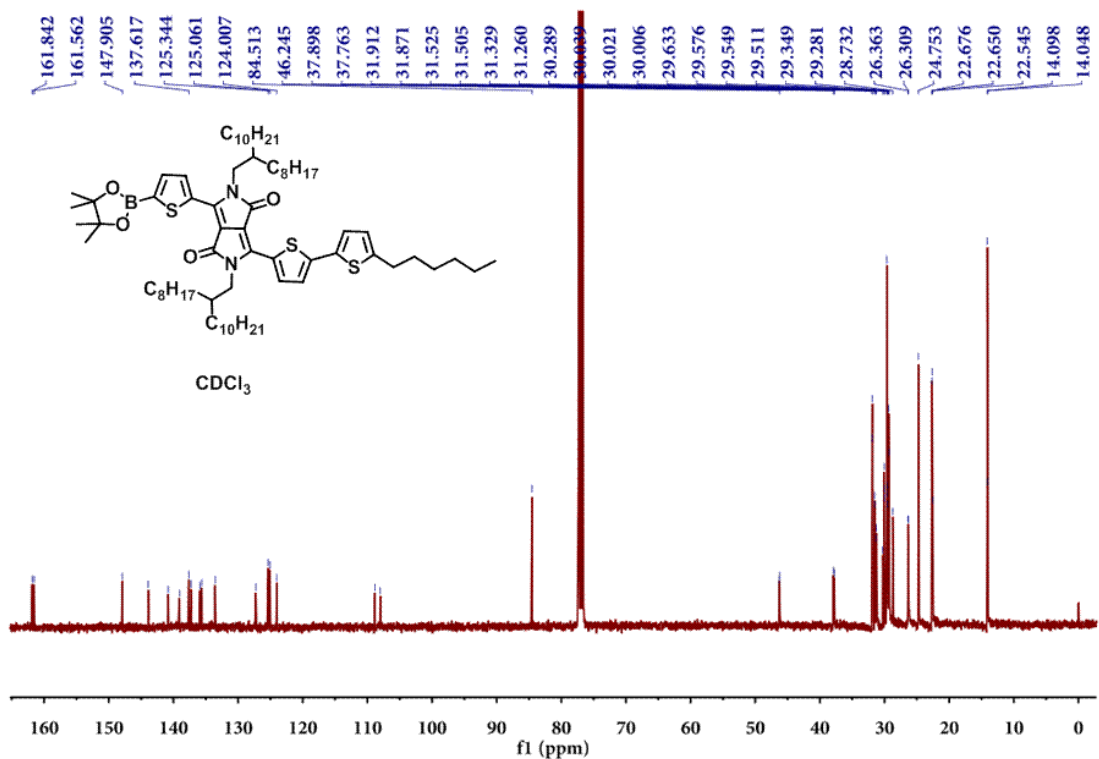
### <sup>13</sup>C NMR of DPP-T (Zoom)



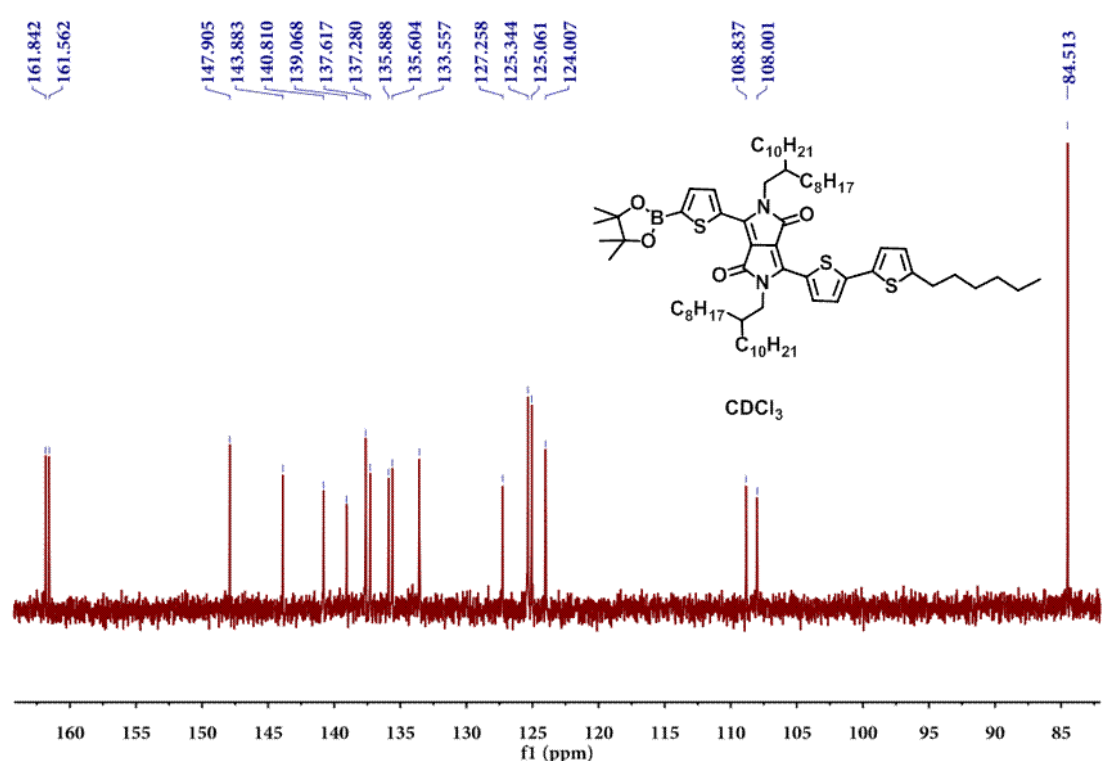
$^1\text{H}$  NMR of **B-DPP-T**



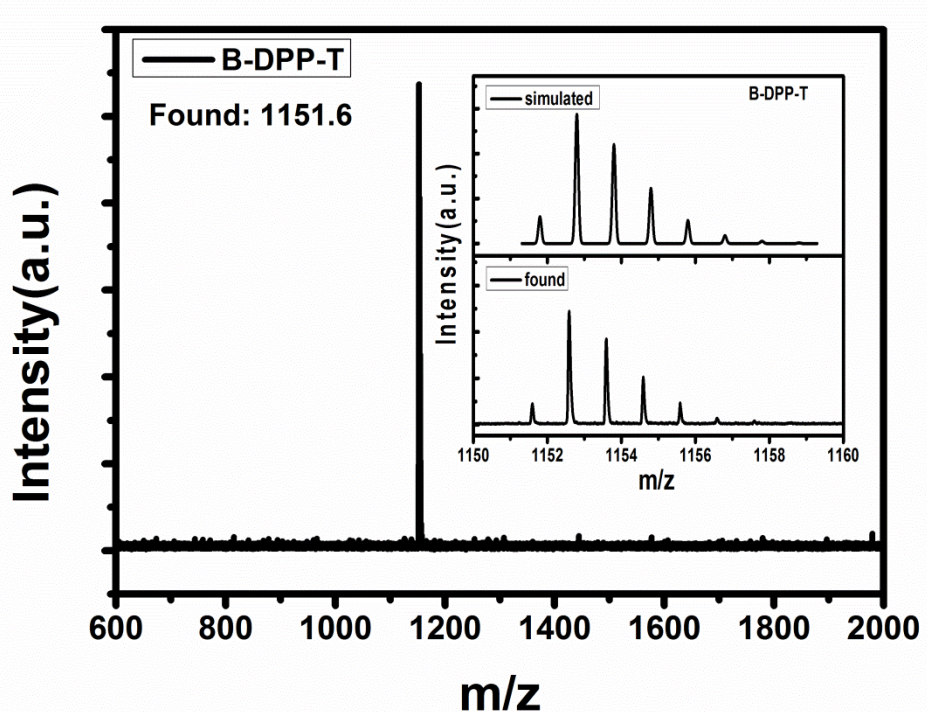
$^1\text{H}$  NMR of **B-DPP-T** (zoom)



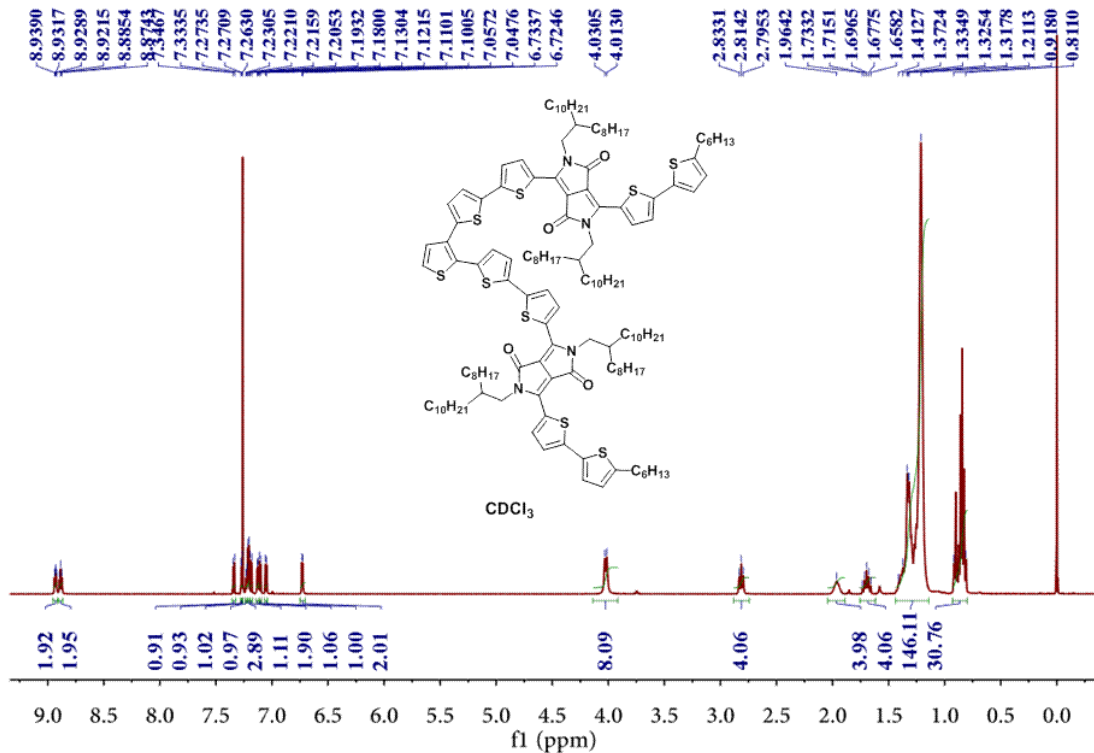
$^{13}\text{C}$  NMR of **B-DPP-T**



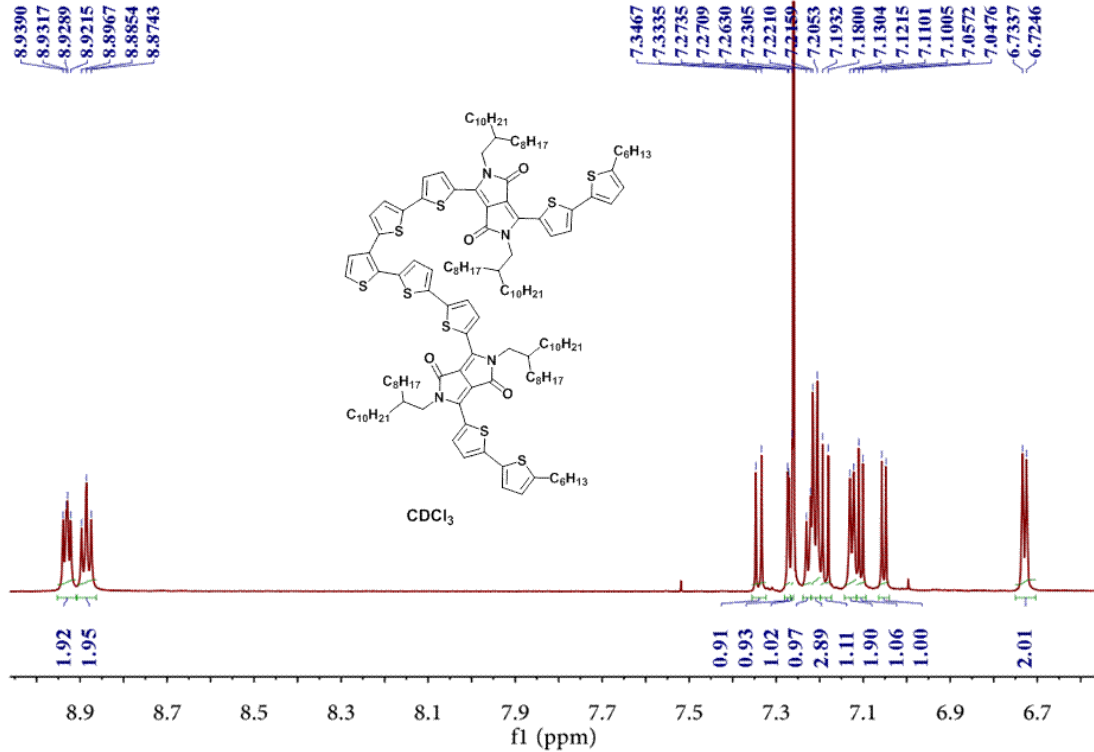
<sup>13</sup>C NMR of B-DPP-T (Zoom)



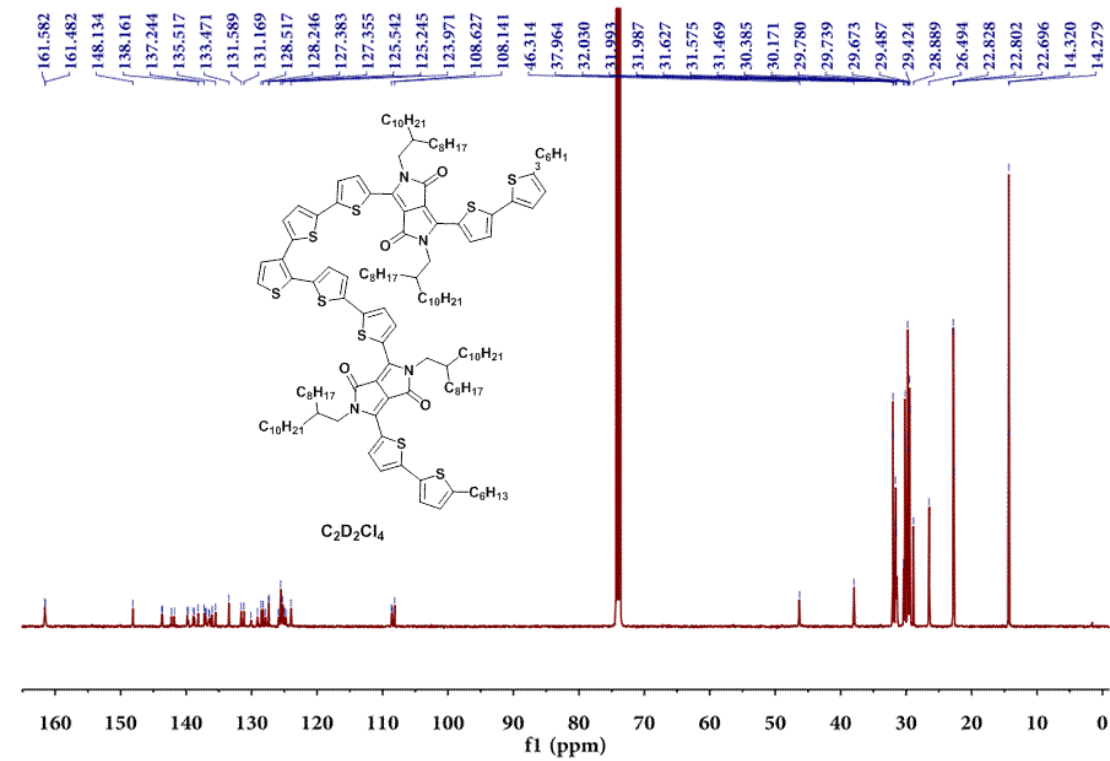
MALDI-TOF MS of B-DPP-T



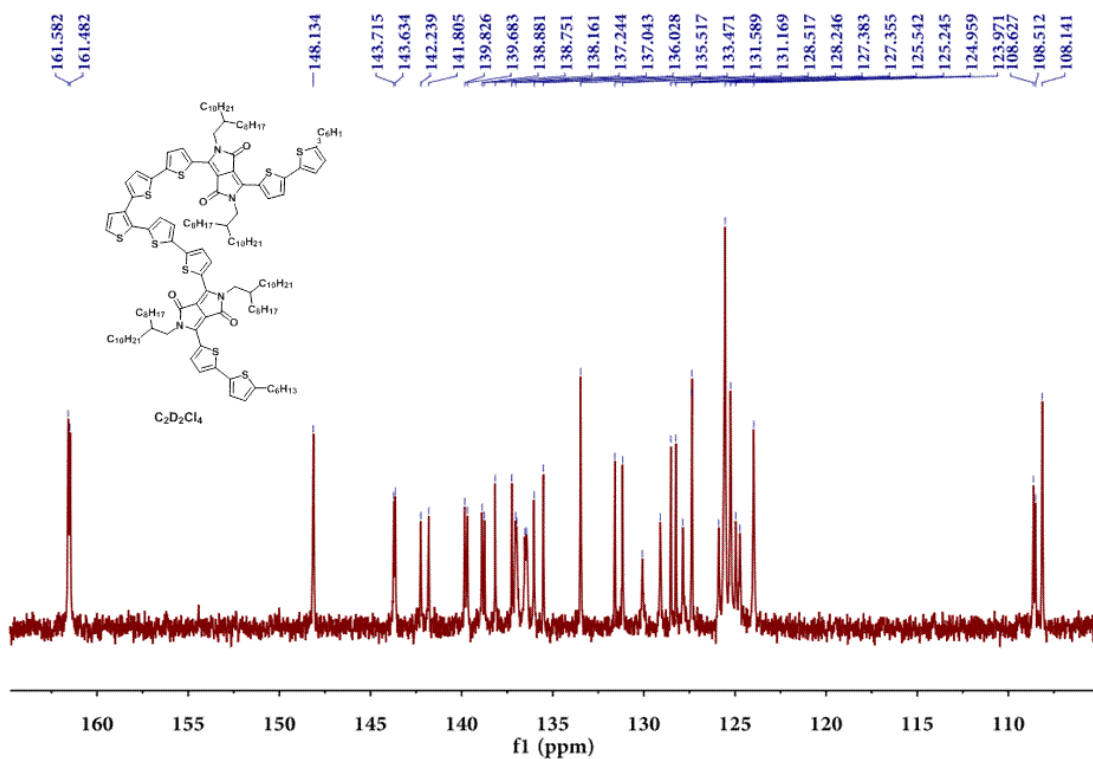
### <sup>1</sup>H NMR of 3T-p-DPP



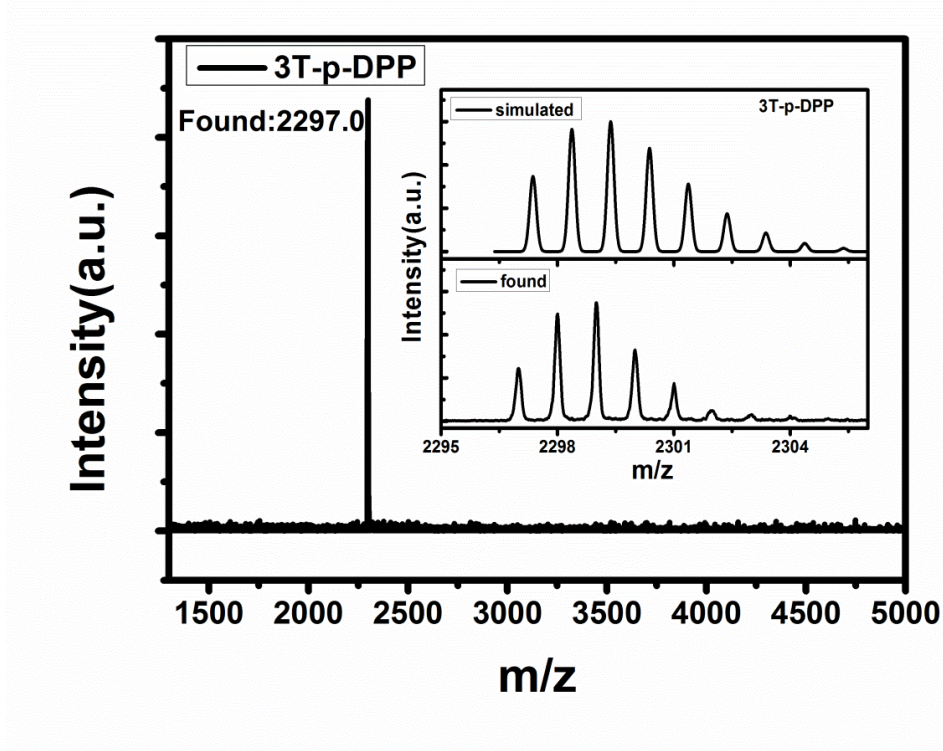
### <sup>1</sup>H NMR of 3T-p-DPP (zoom)



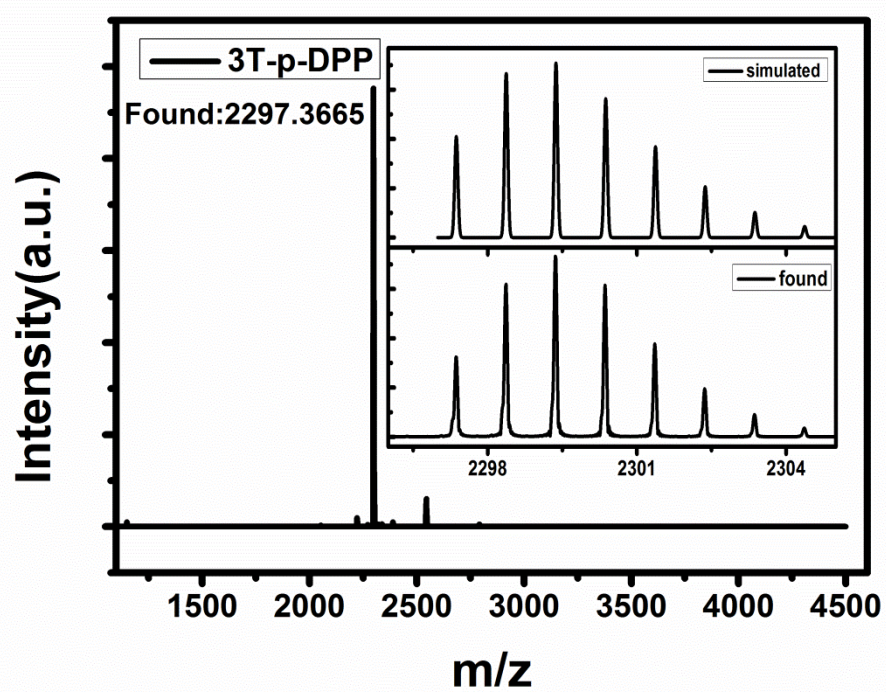
<sup>13</sup>C NMR of 3T-p-DPP



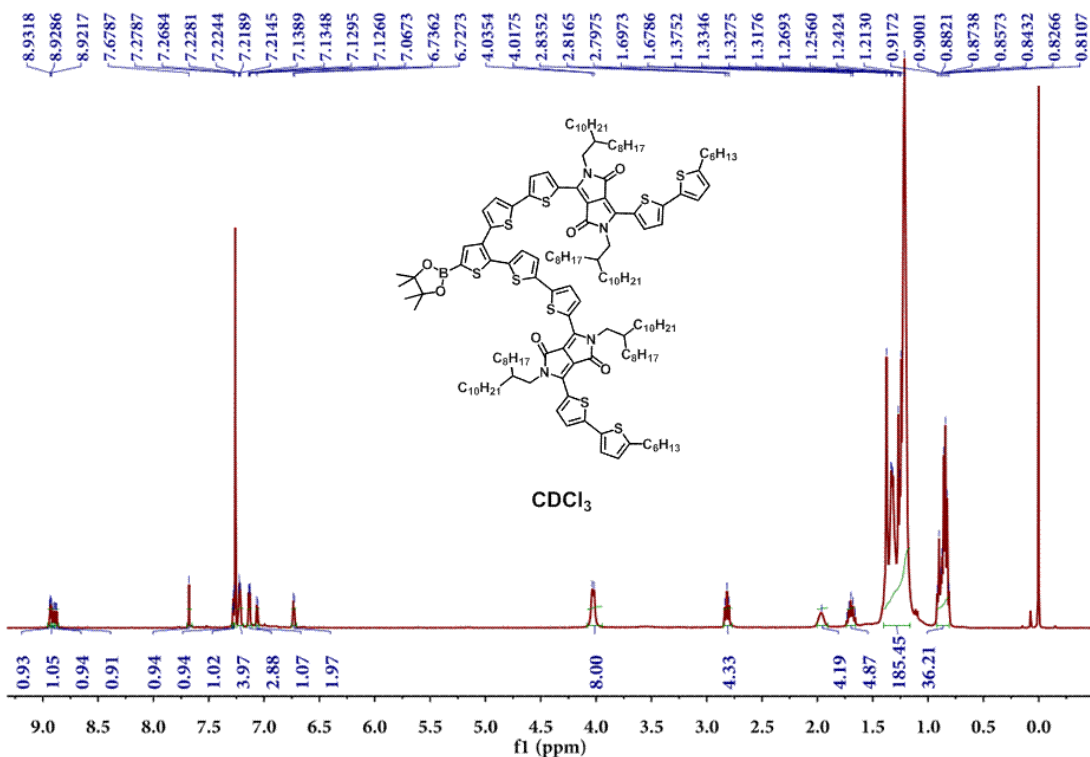
<sup>13</sup>C NMR of 3T-p-DPP (zoom)



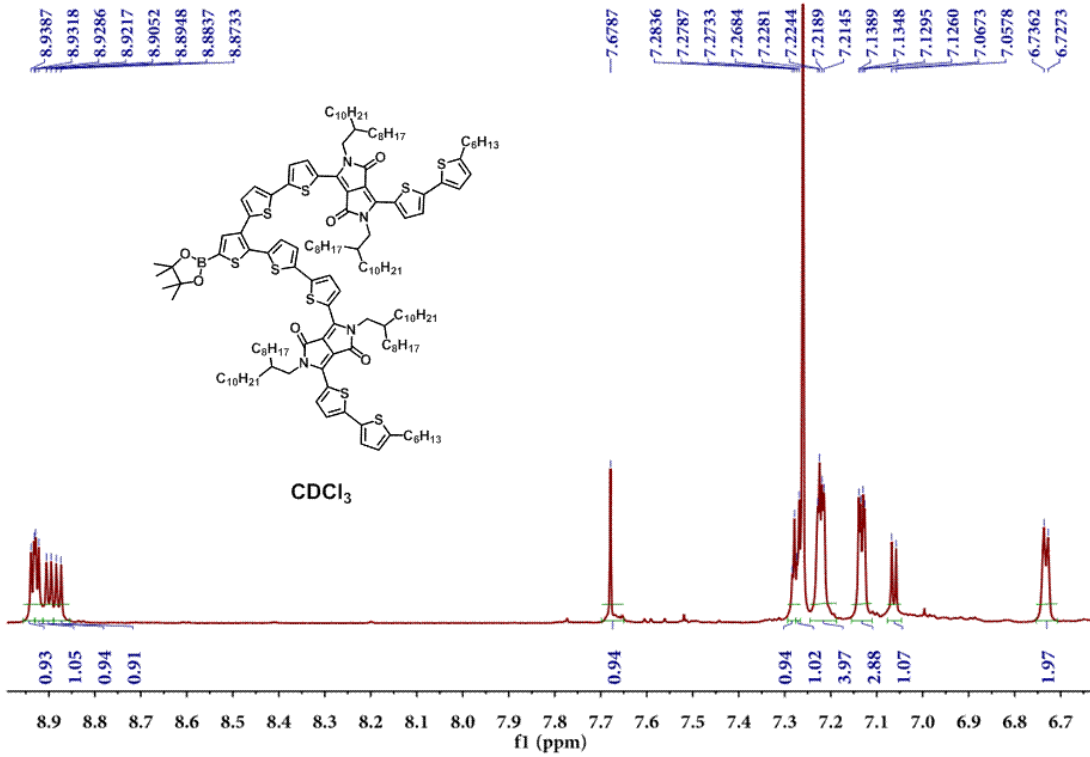
MALDI-TOF MS of 3T-p-DPP



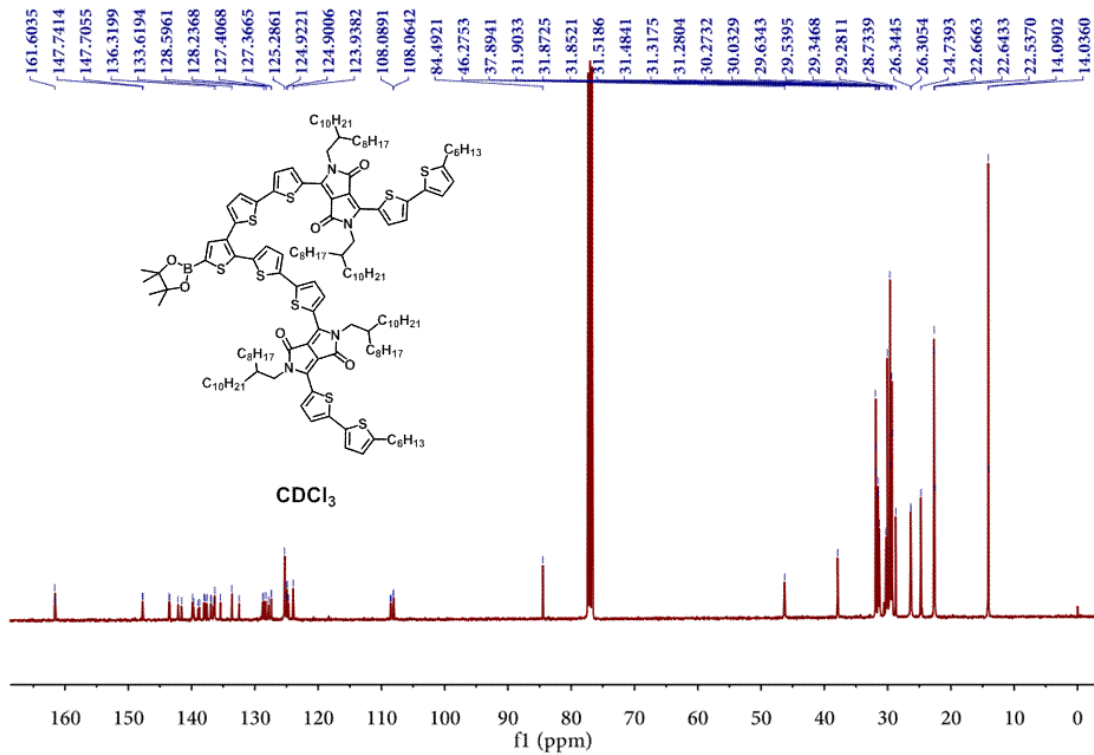
HR MS of 3T-p-DPP



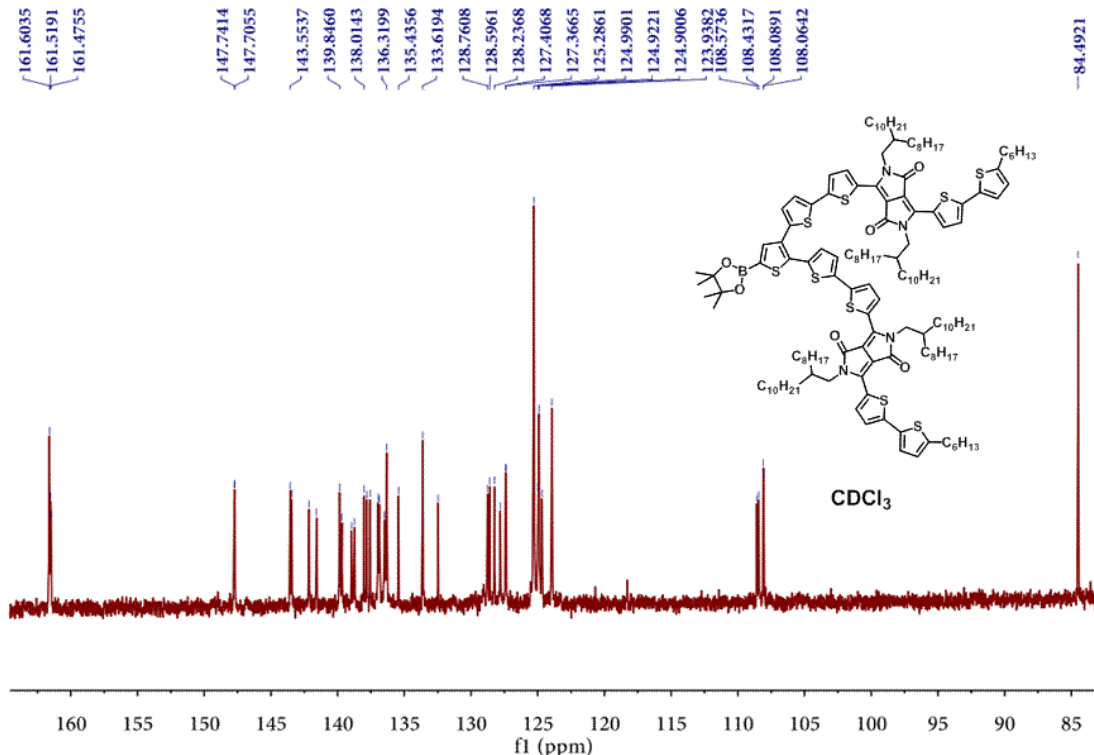
<sup>1</sup>H NMR of B-3T-p-DPP



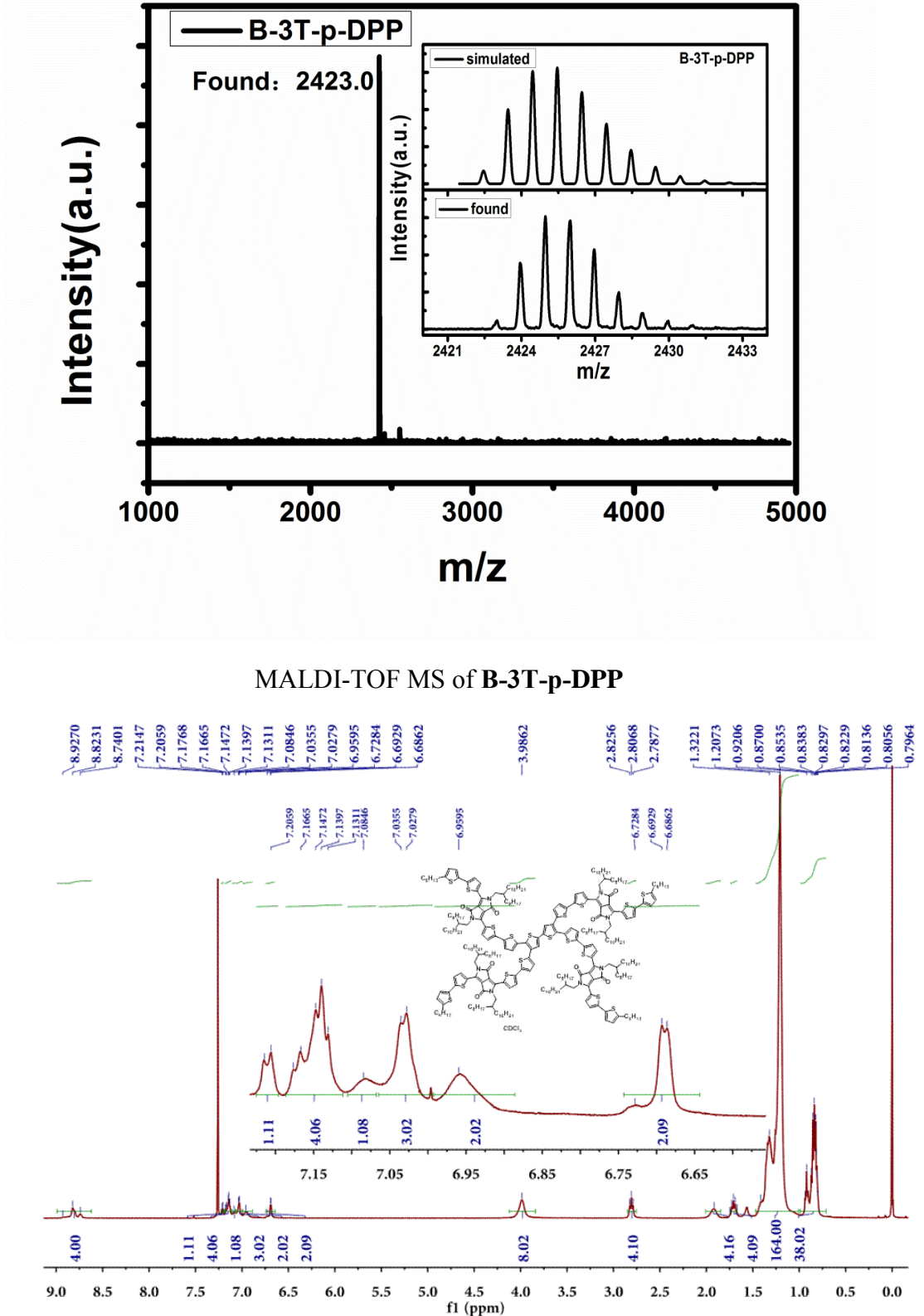
<sup>1</sup>H NMR of B-3T-p-DPP (zoom)



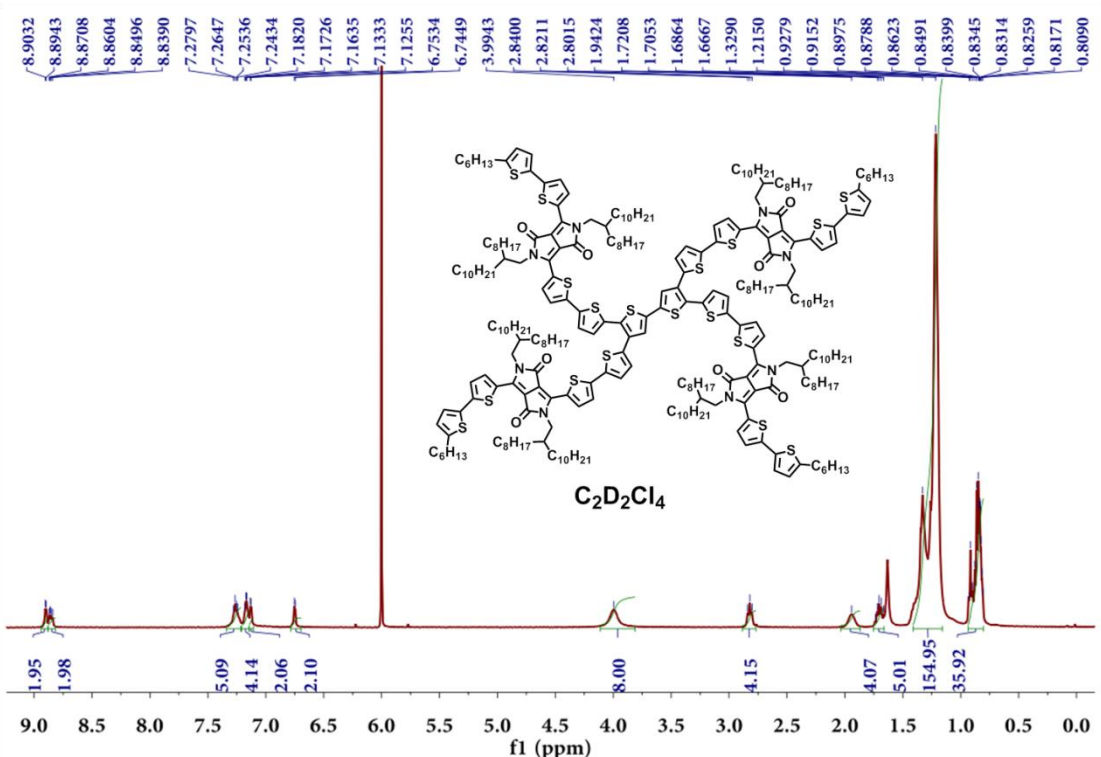
### <sup>13</sup>C NMR of B-3T-p-DPP



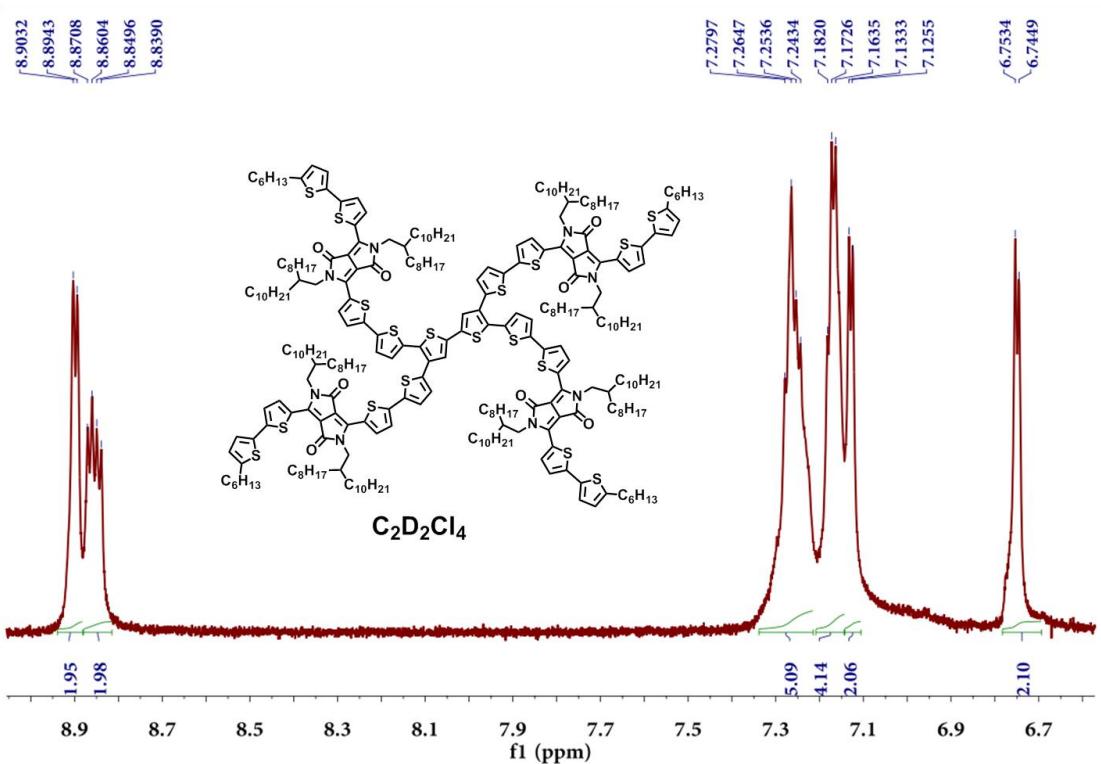
### <sup>13</sup>C NMR of B-3T-p-DPP (zoom)



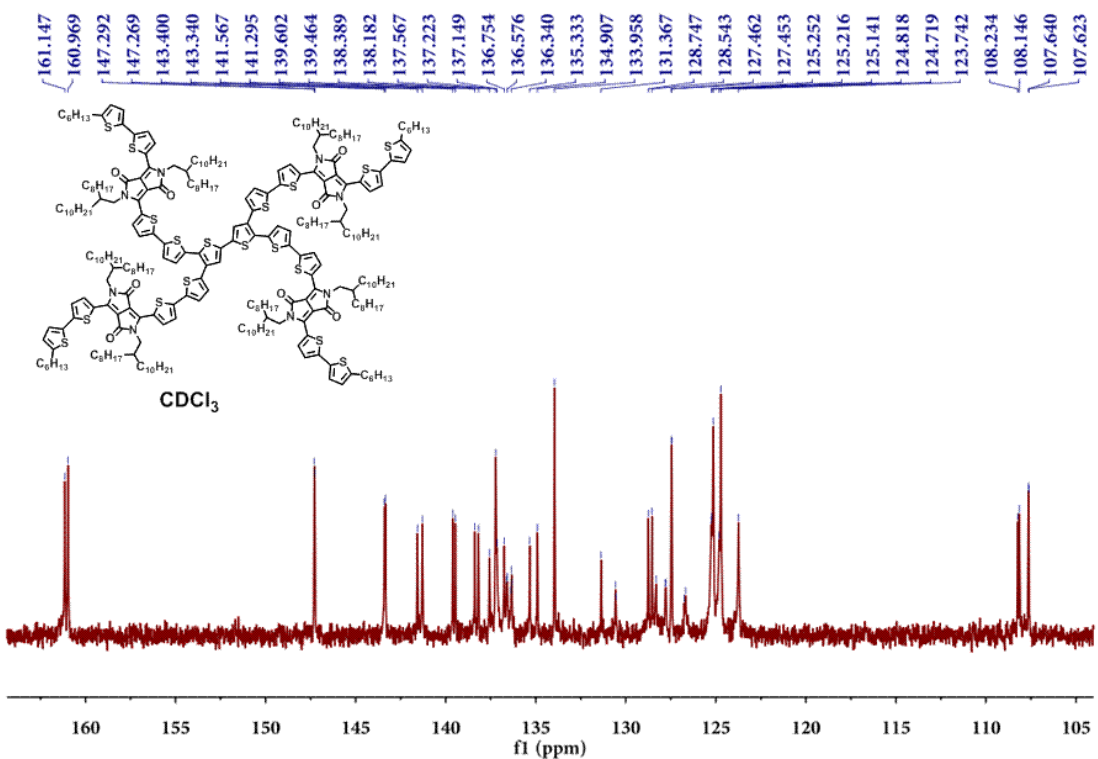
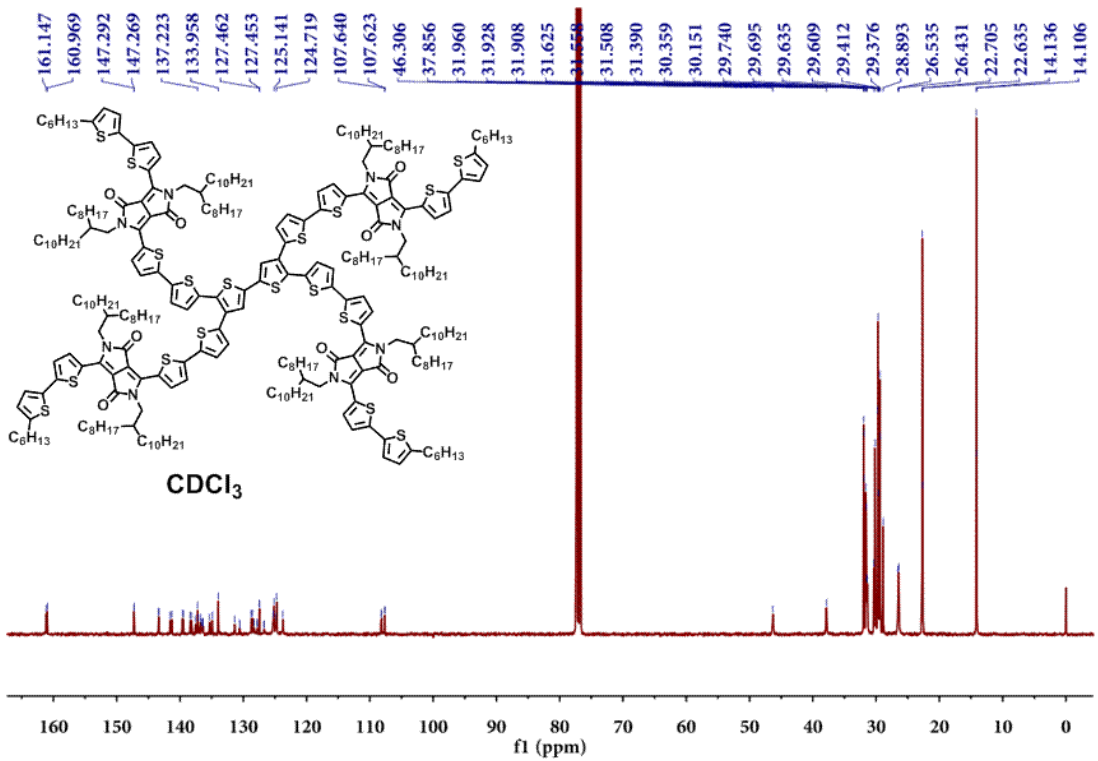
<sup>1</sup>H NMR of 6T-p-DPP ( in CDCl<sub>3</sub>)



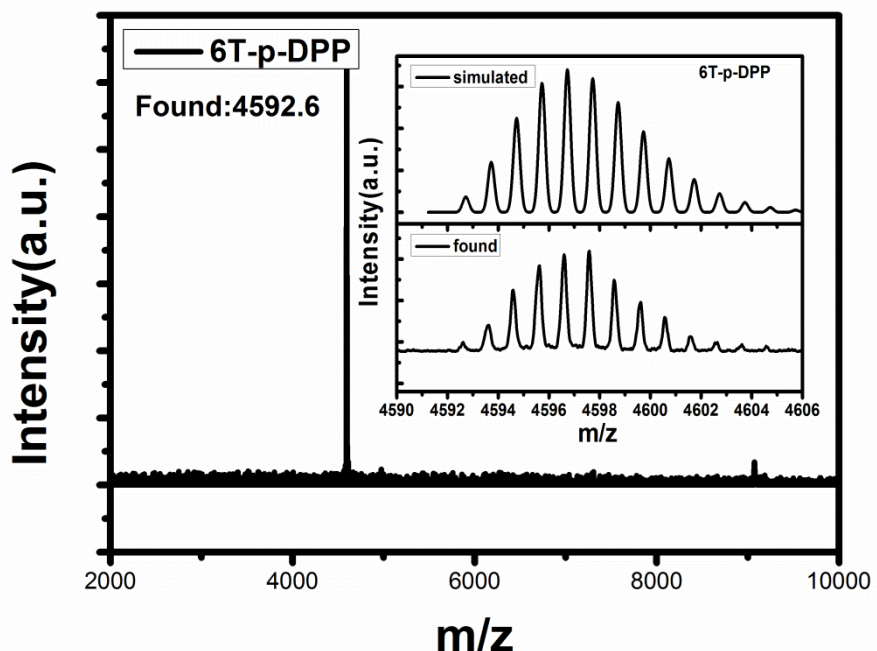
$^1\text{H}$  NMR of **6T-p-DPP**



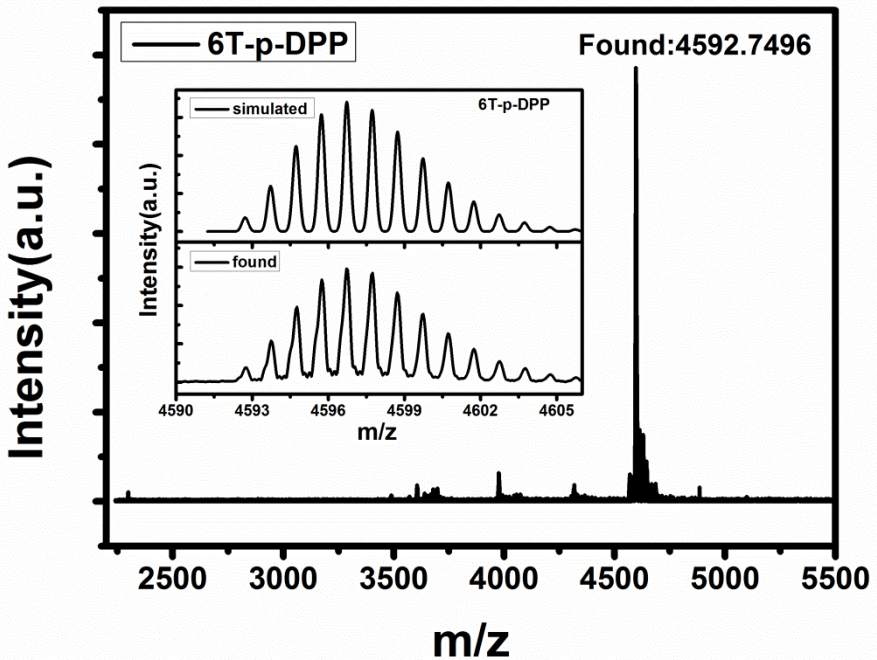
$^1\text{H}$  NMR of **6T-p-DPP** (zoom)



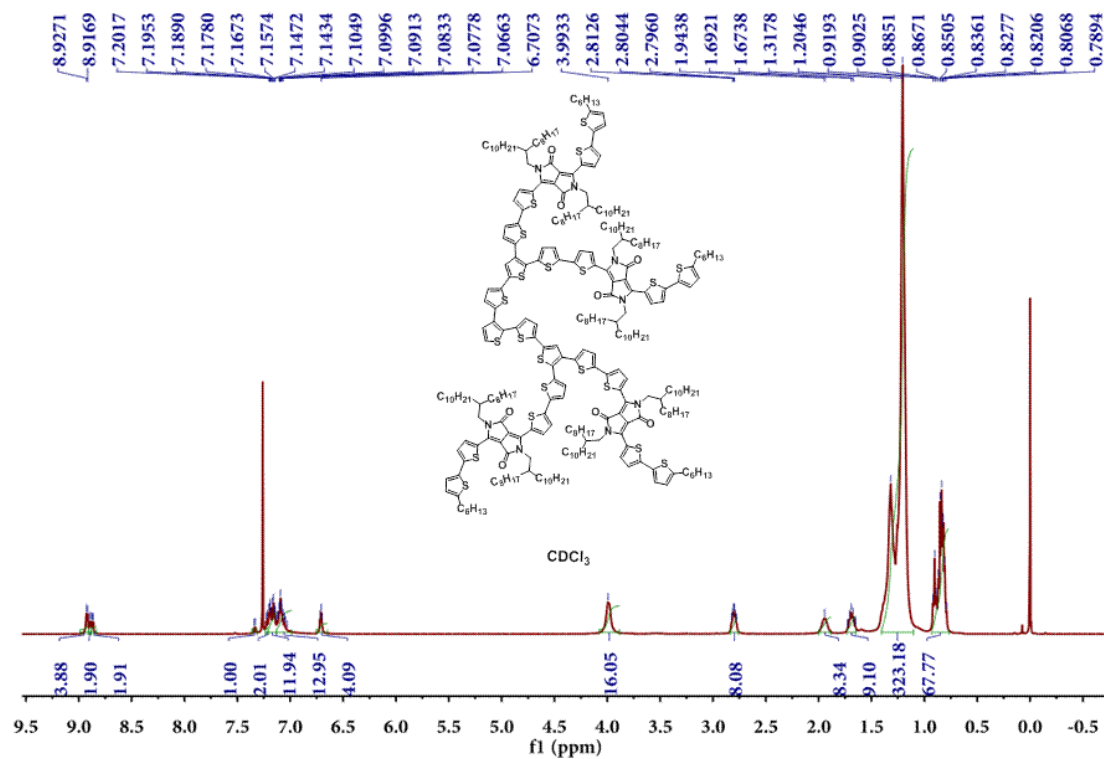
<sup>13</sup>C NMR of **6T-p-DPP** (zoom)



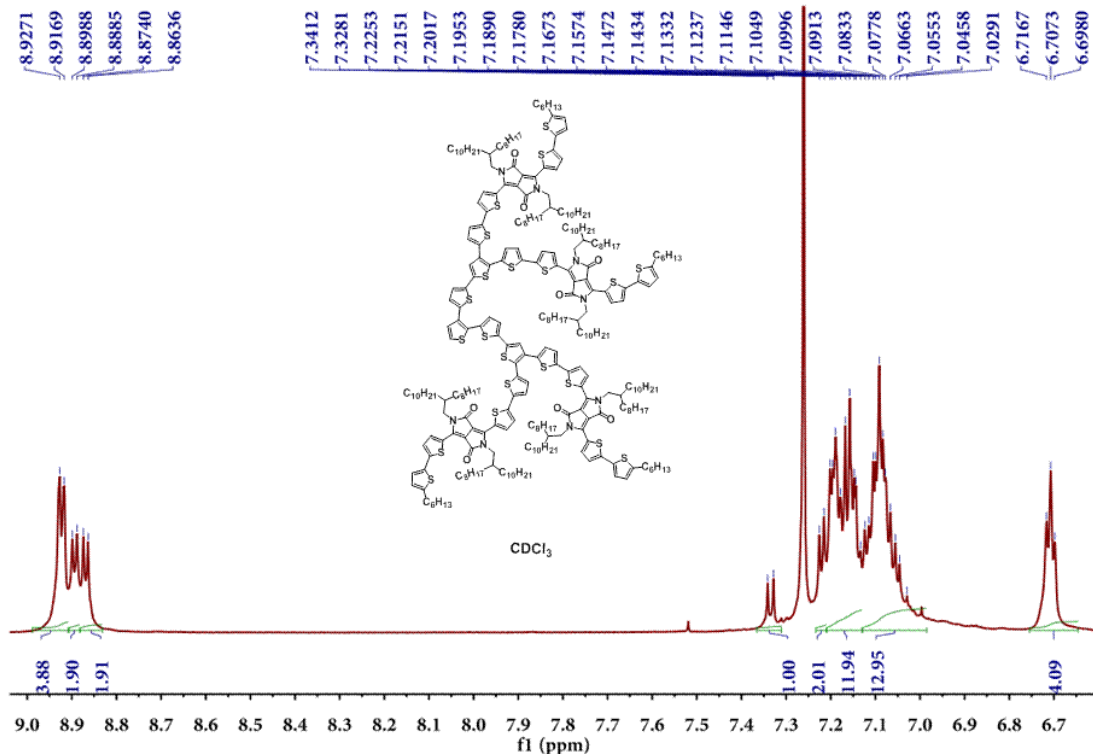
MALDI-TOF MS of 6T-p-DPP



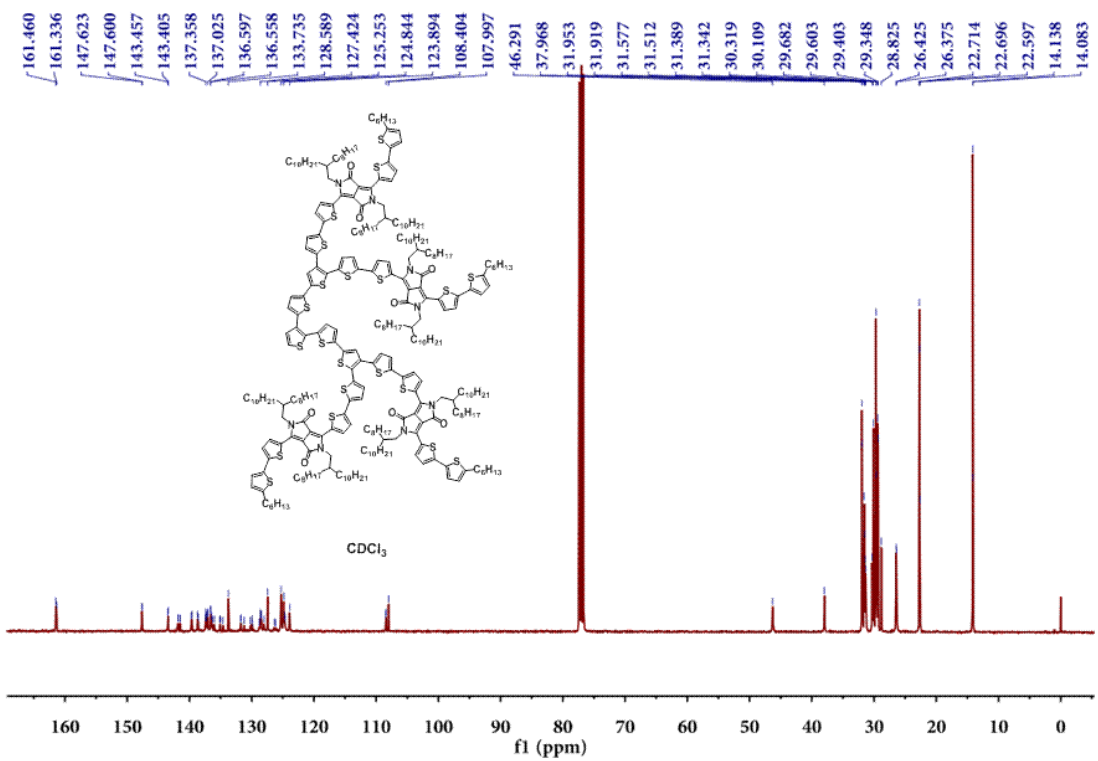
HR MS of 6T-p-DPP



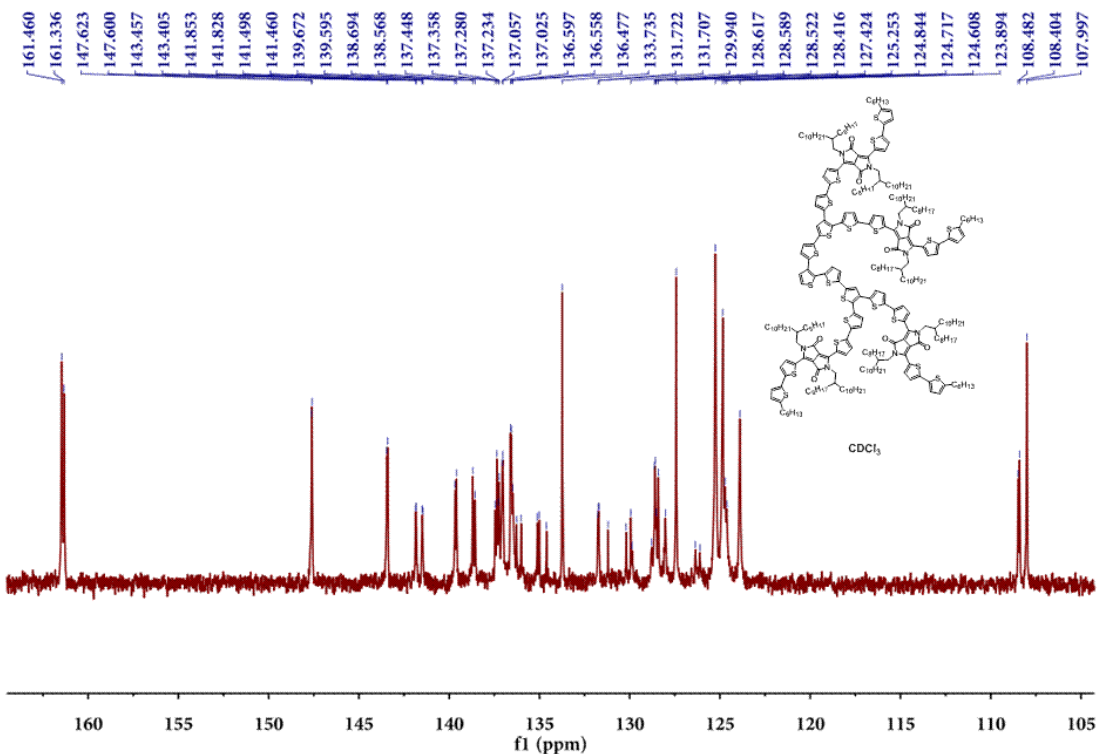
<sup>1</sup>H NMR of 9T-p-DPP



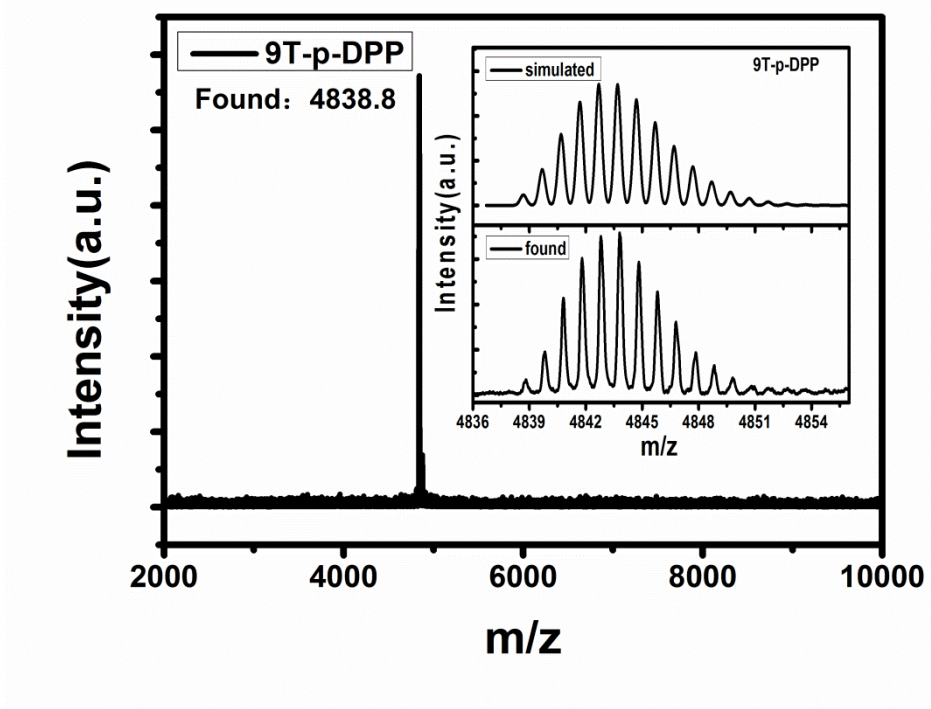
<sup>1</sup>H NMR of 9T-p-DPP (zoom)



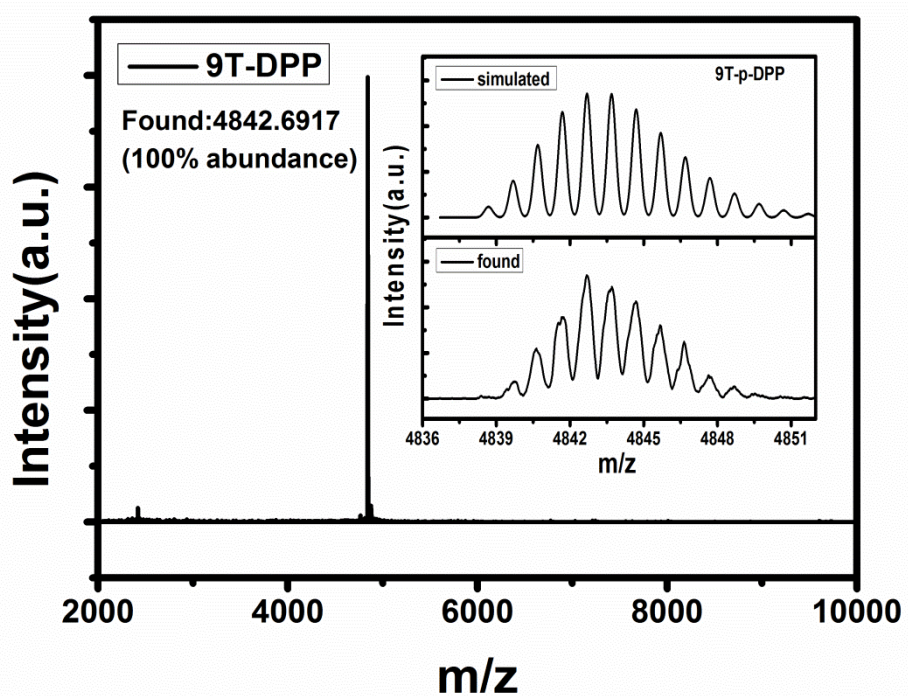
<sup>13</sup>C NMR of 9T-p-DPP



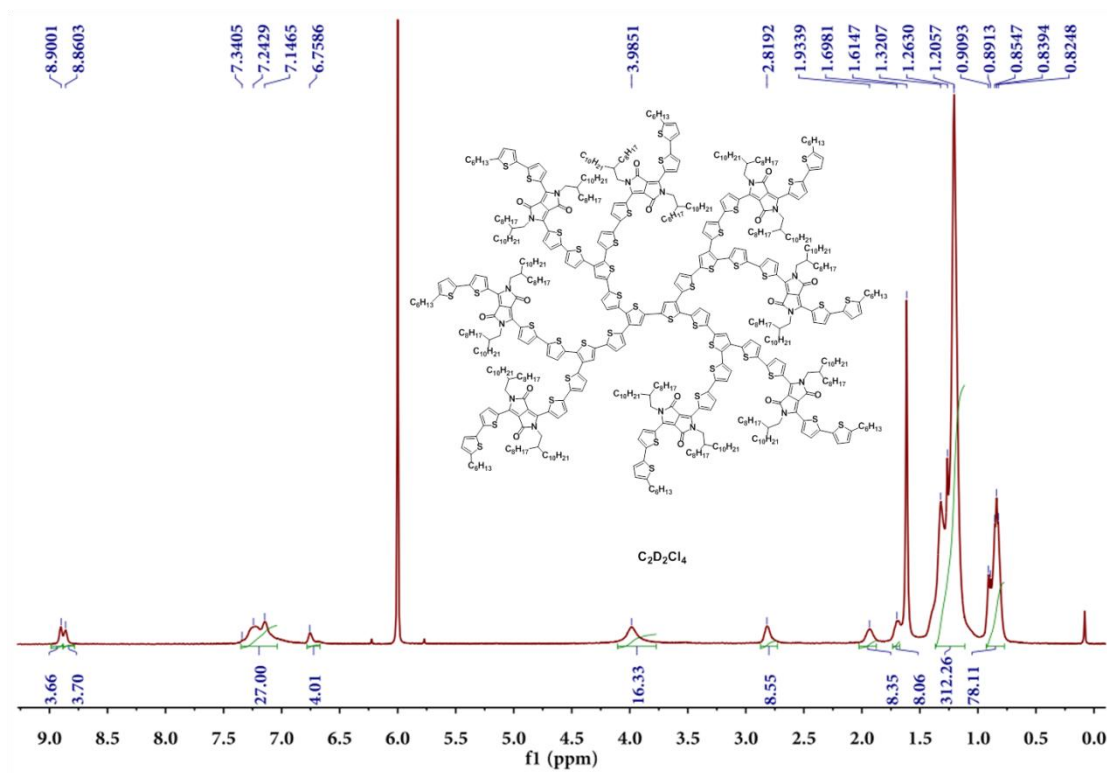
<sup>13</sup>C NMR of 9T-p-DPP (zoom)



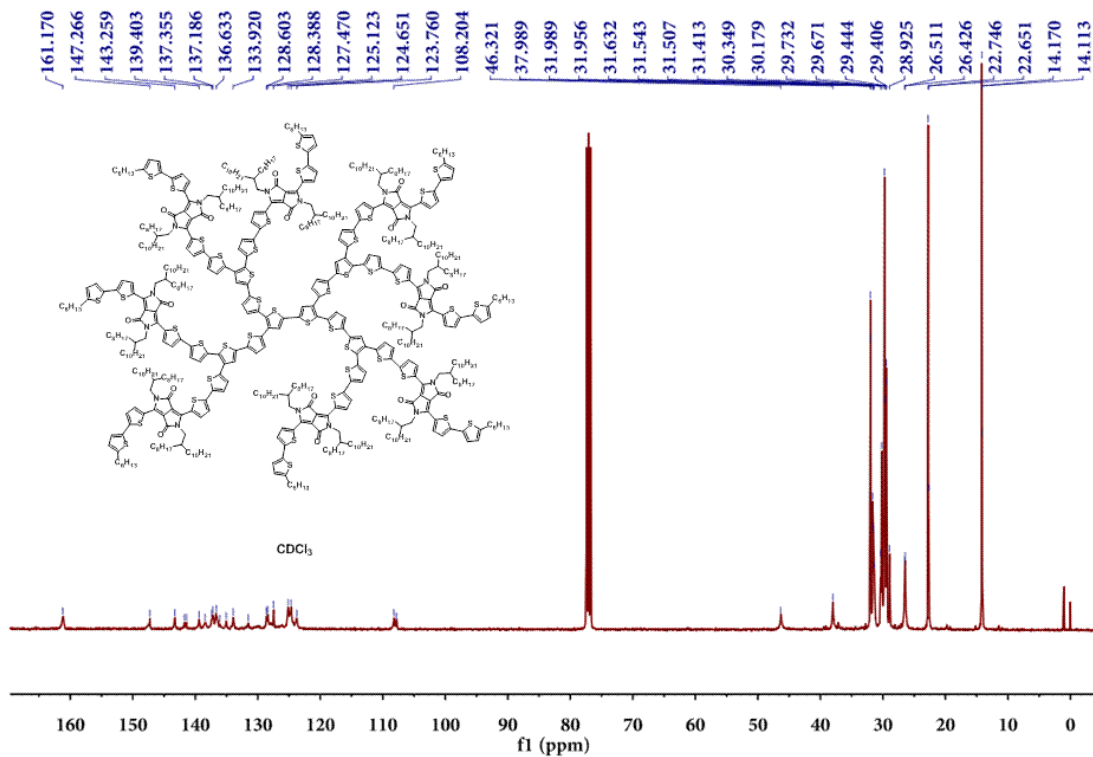
MALDI-TOF MS of 9T-p-DPP



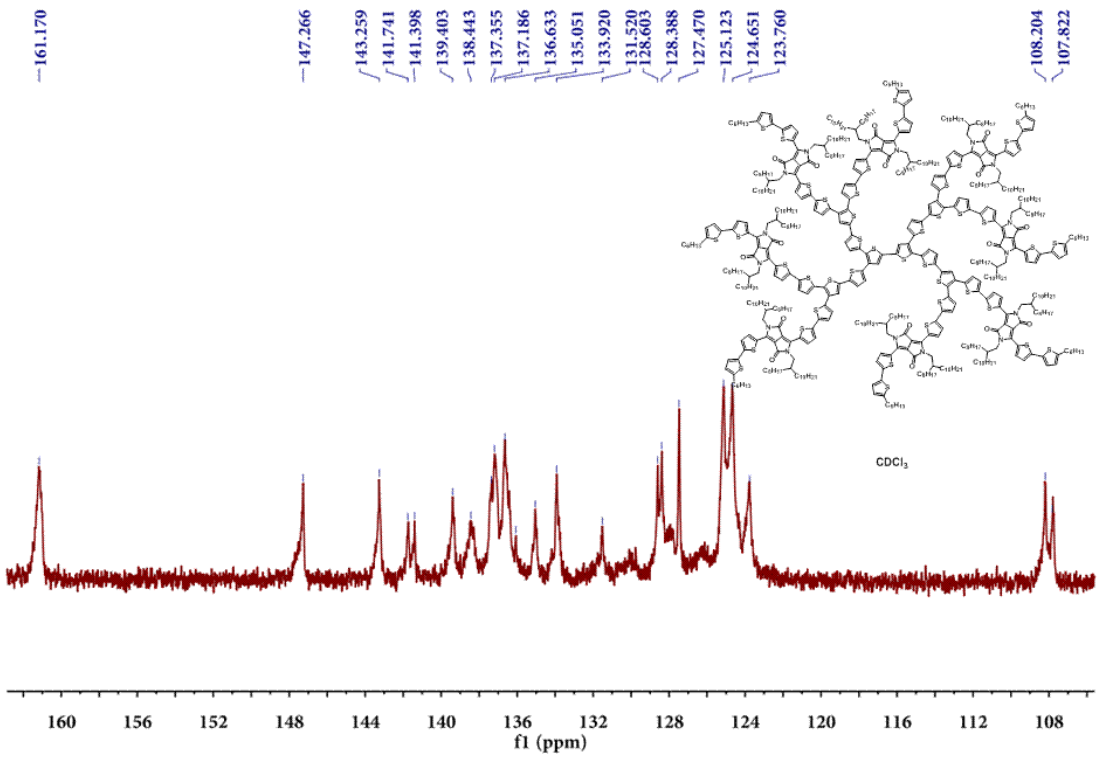
HR MS of 9T-p-DPP



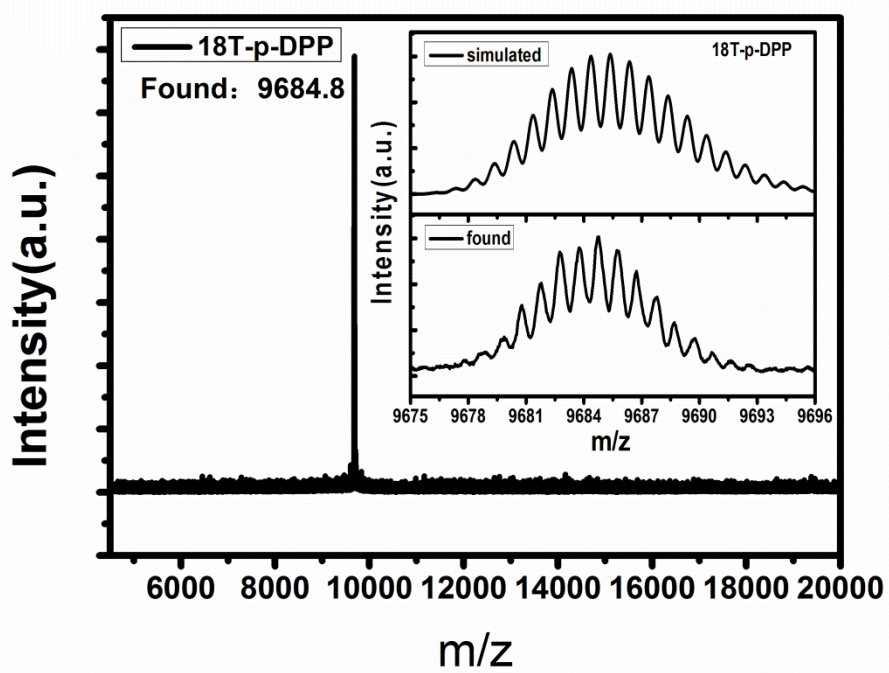
<sup>1</sup>H NMR of **18T-p-DPP**



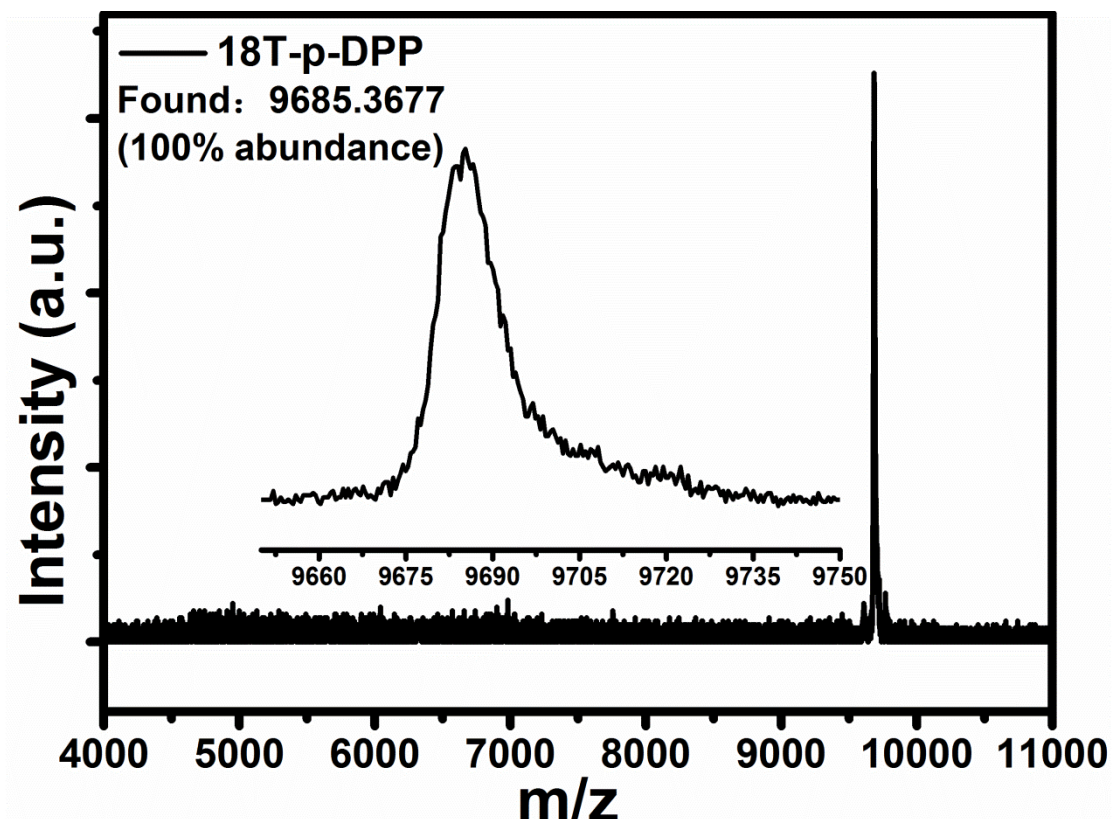
<sup>13</sup>C NMR of **18T-p-DPP**



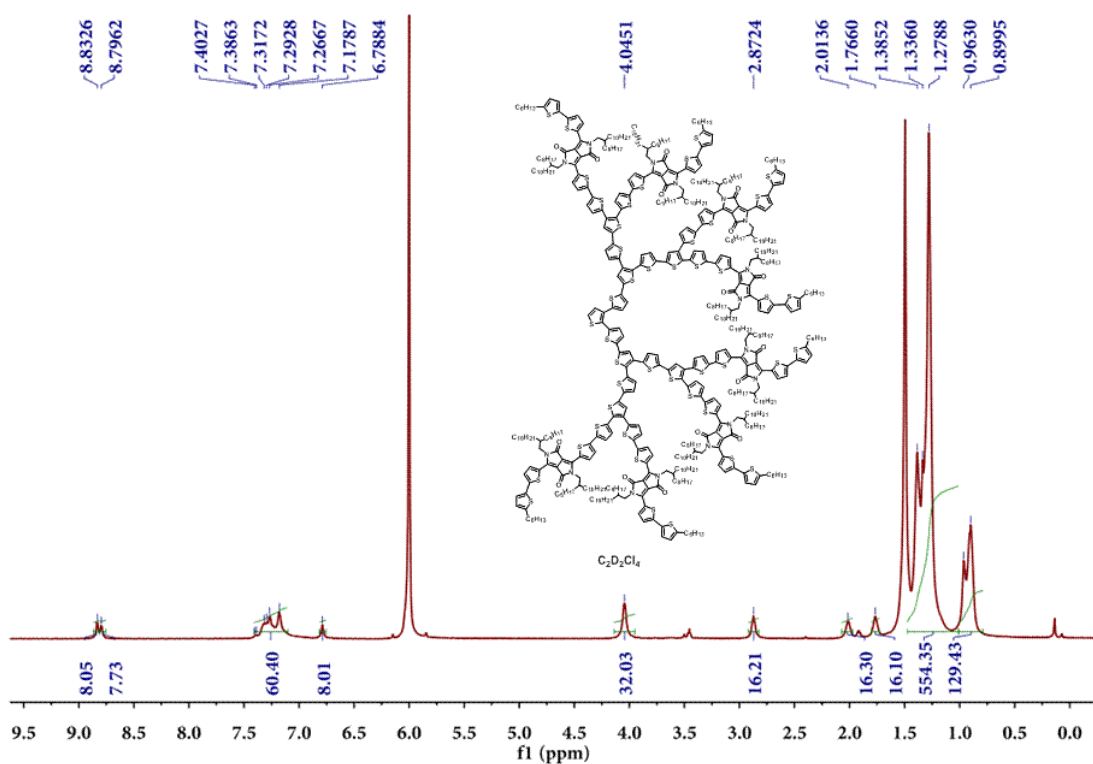
$^{13}\text{C}$  NMR of **18T-p-DPP** (zoom)



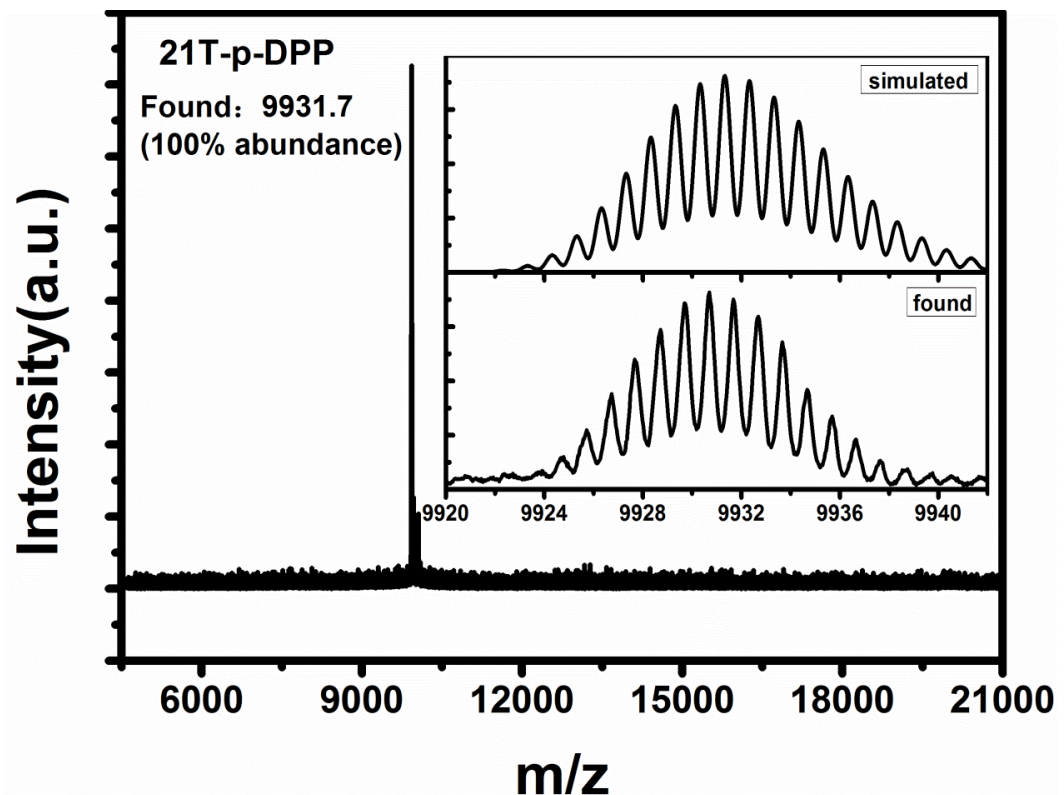
MALDI-TOF MS of **18T-p-DPP**



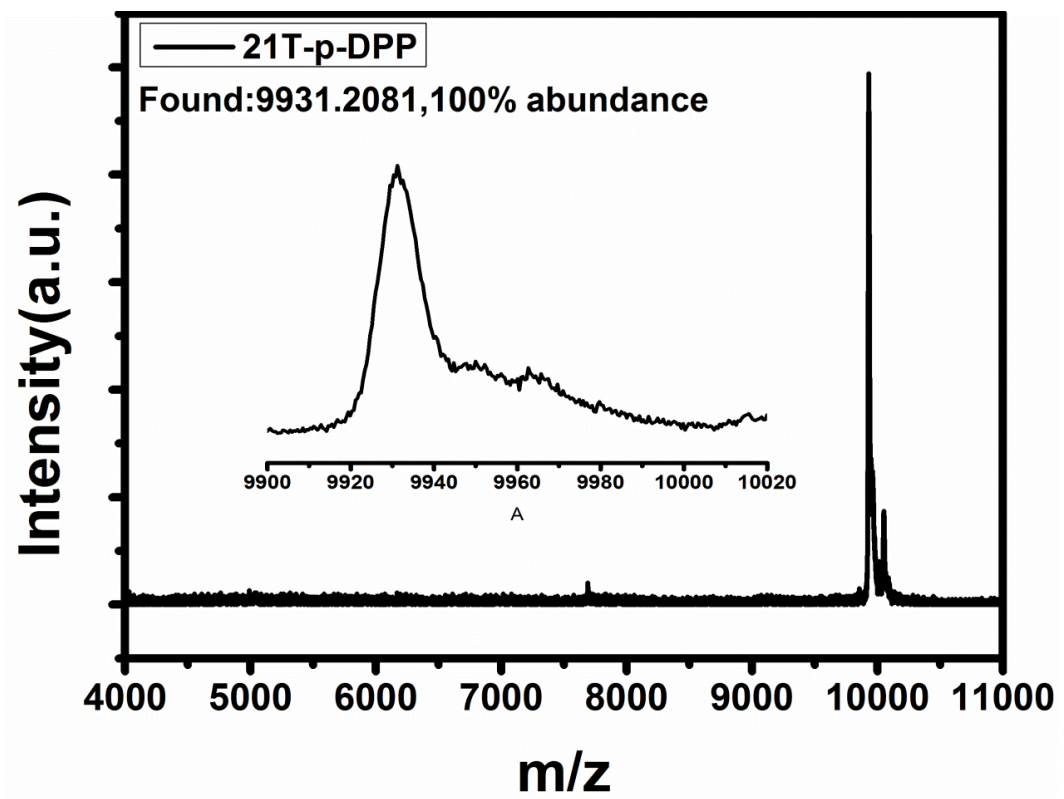
HR MS of 18T-p-DPP



<sup>1</sup>H NMR of 21T-p-DPP



MALDI-TOF MS of 21T-p-DPP



HR MS of 21T-p-DPP